Utrecht University

Physics & Astronomy

Bachelor Thesis

Magnon contribution to unidirectional spin Hall magnetoresistance

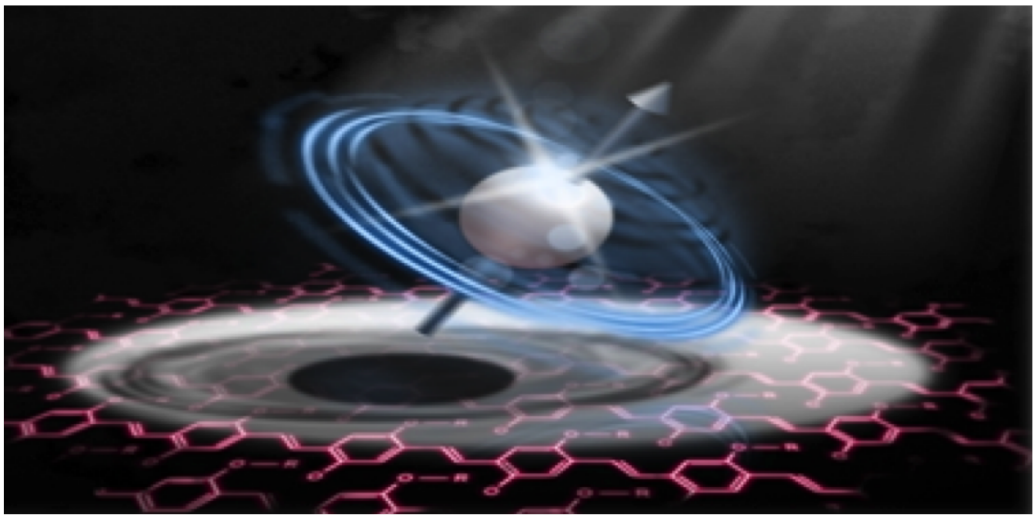

Author
Daan Peerlings

Supervisor
Prof. Dr. R.A. (Rembert) Duine

Institute for Theoretical Physics

June 14, 2017

Abstract

In this thesis, motivated by recent experiments by Avci *et al.* [1], we consider the magnon contribution to the unidirectional spin Hall magnetoresistance (USMR). Zhang and Vignale [2] already considered the electronic contributions to the USMR, accounting for half the experimental findings. Since the electronic contribution is of $\mathcal{O}(\theta)$, where θ is a small parameter, and the magnon contribution of $\mathcal{O}(\theta^3)$, we expect the impact of the magnon contribution on the USMR to be less than that of the electronic contribution. However, we surprisingly find that the contribution of the magnons to the USMR is as large as the electronic contribution.

On the front page we see an artistic representation of an electron spin. The use of the intrinsic angular momentum of the electron and its associated magnetic moment to transfer information extends the field of electronics to that of spintronics. This data transfer via spintronics is portrayed by the stage on which the spin in the picture is spinning. Copyright: http://www.iwavesystems.com/blog/spintronics-a-spin-to-remember/.

Contents

1 Introduction

In this thesis we concern ourselves with spintronics. *Spintronics* is a portmanteau of *spin* and *electronics*. Subsequently, *electronics* itself is a portmanteau of *electron* and *mechanics*. Electronics thus comes down to the study of electrons in order to understand and by extension control their behaviour.

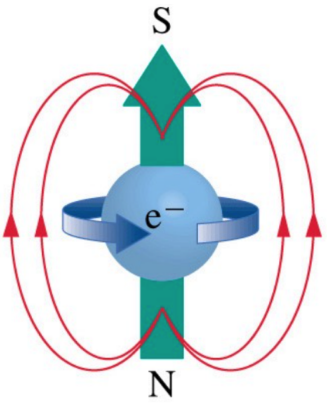

Figure 1: an electron spin represented as an arrow. The intrinsic magnetic moment makes it possible to regard the electron spin as a tiny magnet. Reprinted from Reference [6].

From electronics to spintronics

Since the 1950s, people have used the fact that electrons carry an electric charge to create a charge current which can be adopted for the transport of information. The fundamental building block for this information transport via electronics is the transistor, which has been invented in 1947 by John Bardeen, William Shockley and Walter Brattain [3]. For this invention they received the Nobel Prize in Physics of 1956. The introduction of the transistor led to the Digital Revolution, the transition from the Industrial Age into the Information Age.

In the middle of the Digital Revolution, Intel co-founder Gordon Moore predicted that the number of transistors that would be able to fit on a dense integrated circuit would double yearly [4]. Ten years later, in 1975, he adjusted his prediction from a doubling every year to a doubling every two year [5]. This prediction proved to be accurate over the next decades and is at present day known as Moore's law.

However, since technology has reached the nano-scale regime, the loss of electric energy due to conversion into heat whenever a charge current flows through a resistance has become problematic. That is to say that the moving of the electrons, which is the very base of electronics, poses a problem. At this point, spintronics comes into play.

Spintronics differs fundamentally from electronics. Where in the application of electronics the electric charge is relied upon, spintronics exploits a further degree of freedom of the electron; its spin. The electron spin is the intrinsic angular momentum carried by an electron (as opposed to its angular momentum arising from an orbital motion). An electron spin can only take on one of two opposite values ($\hbar/2$ or $-\hbar/2$), which are usually depicted as arrows pointing either up or down (see Figure 1).

Now instead of transferring information through a flow of charge, in spintronics information is transported through a flow of spin. How such a spin current can arise from freely moving electrons in metals, we see in Section 2 when we discuss the spin Hall effect.

Magnons

Just as an electrically charged body rotating about some axis induces a magnetic field according to classical electrodynamics, so does an electron bear a (spin) magnetic moment proportional to the spin of the electron. This intrinsic magnetic moment allows us to consider the spins as tiny magnets (also see Figure 1).

Given an atom, depending on the element, the outer shell of the atom can either be completely filled with electrons or only partially. If the outer shell is completely filled, the net magnetic moment of the atom is zero (the electron spins cancel each other out). If the outer shell is partially filled, the atom itself may acquire a magnetic moment, making the material as a whole magnetic. Therefore, one model of magnetic materials simply consists of a lattice of spins. The ferromagnetic configuration is a simple example of such.

Figure 2: one-dimensional model of a ferromagnet. In (a) we see the ground state of the ferromagnet. In (b) we see the lowest energy excitation which is a spin wave. The longer the wavelength the less energy the magnon carries. Copyright: Addison-Wesley 2000.

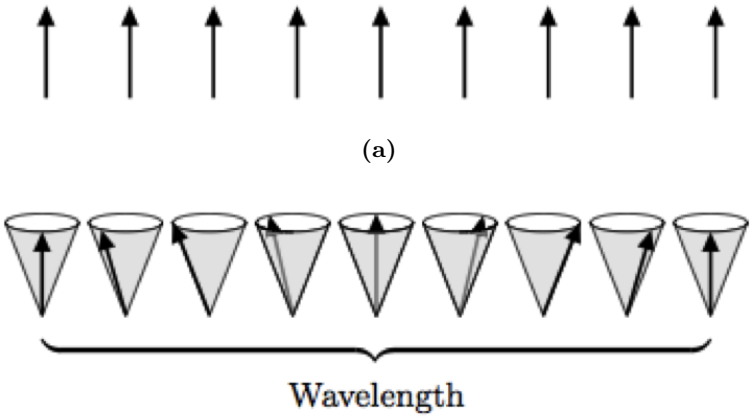

(a)

(b)

In a ferromagnet the magnetic moments of the spins tend to align. In other words, neighbouring spins favour to point in the same direction. At zero temperature, all spins would indeed find themselves in their favoured position. We would then say that the magnet is in its ground state as is depicted in Figure 2a. However, at nonzero temperatures the spins are thermally excited.

One way to excite the ground state is simply by flipping one (or any number) of the spins upside down. Since in a ferromagnet neighbouring spins would ideally be aligned with one another, this kind of excitation leads to an energy increase that is relatively high. We may then ask ourselves the question whether or not there is another way of exciting the ground state, possibly leading to smaller energy increases of the ground state energy. Even more so, the type of excited state acquired through flipping spins is not even allowed quantum mechanically i.e. these states do not form eigenstates of the quantum mechanical Hamiltonian belonging to a ferromagnetic system.

It turns out that there is another way of exciting the ground state. This is by so-called spin waves which can be imagined to look like Figure 2b. Excited states of this kind indeed do form eigenstates of the quantum mechanical Hamiltonian. Very impromptu, we might have expected spin waves to be the correct form of excitation because of the wave-particle duality in quantum mechanics. Moreover, exciting the ground state through spin waves leads to energy increases that are much less than those we find by flipping spins.

In Section 3 we make this explicit and see how quantized spin waves, called magnons, arise in ferromagnets. Note that, although there are many forms of magnetism, throughout this thesis we only consider the ferromagnetic kind. The magnons are able to carry a spin current themselves (just as the free electrons in a conductor). We thus have two types of spin currents; one carried by valence electrons in a metal, the other by magnons in a (ferro)magnet (see Figure 3).

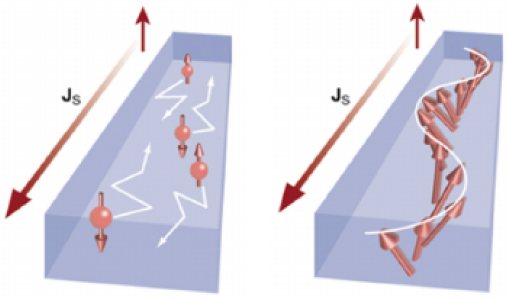

(a) **(b)**

Figure 3: spin currents. In (a) we see a spin current carried by valence electrons in a metal. In (b) we have a spin current carried by magnons in a ferromagnet. Reprinted from Reference [7].

Unidirectional spin Hall magnetoresistance

In Section 4 we consider a bilayer of a nonmagnetic metal and a ferromagnetic insulator (denoted as NM/FM bilayer). In the nonmagnetic metal we then have an electron spin current which, at the interface between the layers, is converted into a magnon spin current in the ferromagnetic insulator. Across the interface then appears an interfacial spin current. This interfacial spin current we calculate up to and including second order in the electron spin accumulation and the magnon spin accumulation.

We do this in response to recent experiments performed by Avci *et al.* [1]. In a NM/FM bilayer they have measured a magnetoresistive effect, named the unidirectional spin Hall magnetoresistance, that changes when the direction of the magnetization in the ferromagnet is inverted. Normally, magnetoresistive effects are invariant on inversion of the magnetization direction. In Section 5 we go into more detail on the unidirectional spin Hall magnetoresistance (USMR) and introduce a characterization of its amplitude:

$$\text{USMR} = \frac{\rho(E) - \rho(-E)}{\rho(E)}\,, \tag{1.1}$$

where ρ is the longitudinal resistivity of the nonmagnetic metal and thus explicitly depends on (the direction of) the electric field E.

So far, the experimental observations have not been given a definitive interpretation. Zhang and Vignale [2] made an effort to explain the nonlinear magnetoresistance considering only the electronic contribution to the unidirectional spin Hall magnetoresistance. Their result accounted for half the experimental value. In this thesis, we consider the magnon contribution. The magnon contribution to the USMR is of $\mathcal{O}(\theta^3)$, where θ is a small parameter. Hence we expect this contribution to be of less importance than the electronic contributrion which is of $\mathcal{O}(\theta)$ [2]. In the end however, we conclude that the magnon contribution to the USMR is not negligible relative to the electronic contribution.

Organization of thesis

The remainder of this thesis is organized as follows. We start in Section 2 with discussing electrical conductivity in metals via the Drude model. In Subsections 2.1 and 2.2 we first review the (classical) Hall effect and then consider the spin Hall effect. In Section 3 we introduce the concept of magnons as quantized spin waves in ferromagnets. We do so semi-classically as well as quantum mechanically. Having introduced the spin Hall effect and magnons, we regard a bilayer of a nonmagnetic metal and a ferromagnetic insulator in Section 4. The bilayer structure leads to certain effects, of which we examine the interfacial spin current in detail. This interfacial spin current allows us to solve for the characterization of the magnitude of the USMR (1.1), as is explained in Section 5. In Section 5 we finally consider a bilayer of platinum and yttrium iron garnet to substitute numerical values for the parameters. In this way we find the dependence of the USMR on the thickness of the ferromagnet and on the temperature. We discuss results in Section 6.

2 Nonmagnetic metals

First of all, we consider nonmagnetic metals. In Subsections 2.1 and 2.2 we get into the workings of the classical Hall effect and the spin Hall effect respectively. Before we do so, we first examine a simple model of electrical conduction proposed by Paul Drude in 1900 [8]. The discussion of this model and that of the classical Hall effect rest on Reference [9]. The derivations that eventually elicit the spin Hall effect come from Reference [10].

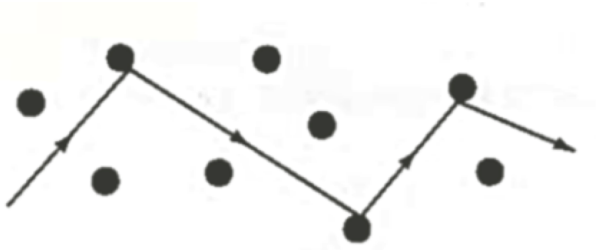

Figure 4: the Drude model. The path an electron might follow in a metal. In between the ions, the electron moves in a straight line. On the ions the electron scatters randomly. Reprinted from Reference [9].

In the Drude model, the kinetic theory of gases is applied to metals. Metals are thus considered to consist of a gas of electrons. The simplest of kinetic theories treats the particles of a gas as identical hard spheres. Between the hard spheres there are no forces present other than the infinite repulsion at the moment the spheres would otherwise overlap. In between these collisions then, the spheres simply move in straight lines.

Where in normal gases the particles of the gas can be of one kind only, for a metal we need at least two different kinds of particles. After all, the electrons are negatively charged whereas the metal as a whole is electrically neutral. This makes the presence of positively charged particles necessary. Hence, we will model the metal as follows. Whenever metallic atoms are brought together to form a metal, the valence electrons detach themselves from the atoms and will move freely through a static lattice of what are now positively charged ions (see Figure 4).

Due to the presence of electronic charges and a static lattice of ions, this model calls for slight modifications of the kinetic theory for neutral dilute gases. We will briefly state the basic assumptions of the Drude model. First of all the *independent electron approximation* is adopted, which simply states a neglect of electron-electron interactions. Also we adopt the *free electron approximation*, neglecting electron-ion interactions. (This is not entirely true since we do take into account scattering processes and confine the electrons to the metal. Both of these effects however, have only to do with the mere presence of (a lattice of) ions.) In externally applied electromagnetic fields the electrons therefore simply obey Newton's laws of motion without any additional (complicated) fields originating from the electrons and ions.

As for the collisions, we introduce a relaxation time τ. Relaxation refers to the return of a perturbed system into equilibrium. In the metal, the electrons return to thermal equilibrium for example by colliding with the ions. The collisions provide for this equilibration in the following way. When colliding with an ion, the electron scatters in any (random) direction and with a speed appropriate to the temperature prevailing at the place of collision (i.e. the hotter the place of the collision, the faster the electron will move after the collision). An important aspect of the Drude model is that it does not concern itself with the specifics of the scattering mechanism; it simply assumes that there is *some* mechanism responsible for the scattering, all the details of which are absorbed in the relaxation time. The relaxation time τ denotes the inverse probability per unit time of an electron experiencing a collision. In other words, the probability that an electron collides within an infinitesimal time interval dt is simply dt/τ. This means that, on average, any electron will have travelled a time τ since its last collision and will travel for a time τ until its next collision.

An important application of the Drude theory is the calculation of the DC electrical conductivity of a metal. Newton's second law of motion for the electrons in the metal becomes [9]

$$\dot{\mathbf{p}} = \mathbf{F} - \frac{\mathbf{p}}{\tau}\,, \tag{2.1}$$

where the last term is a frictional damping term which arose from the Drude model. Applying an external electric field $\mathbf{E}$ results in an electric force $\mathbf{F}_{el} = -e\mathbf{E}$ acting on each electron. With $\mathbf{F} = \mathbf{F}_{el}$ and with our system in a steady state (i.e. $\dot{\mathbf{p}} = 0$) we can solve (2.1) for the momentum and find

$$\mathbf{p} = -e\mathbf{E}\tau\,. \tag{2.2}$$

The electric field we introduced, induces a current density $\mathbf{j}$ that is parallel to the flow of charge and whose magnitude is the amount of charge per unit time crossing a unit area perpendicular to the direction of the flow. The current density is therefore given by [9]

$$\mathbf{j} = -ne\mathbf{v}\,, \tag{2.3}$$

where a density of n electrons (of charge $-e$) per unit volume move with velocity $\mathbf{v}$. Introducing the electron mass m we find by combining (2.2) and (2.3) that

$$\mathbf{j} = \sigma\mathbf{E} \text{ where } \sigma = \frac{ne^2\tau}{m}\,, \tag{2.4}$$

establishing a linear dependence of $\mathbf{j}$ on $\mathbf{E}$. Here σ is the DC electrical conductivity we set out to find. However, in our derivation we were only bothered with the presence of an external electric field. Additionally we can subject the metal to an external magnetic field. This is the subject of Subsection 2.1.

2.1 Classical Hall effect

The Hall effect is the production of an electric field across two faces of a conductor in the direction of $\mathbf{j} \times \mathbf{B}$, where $\mathbf{B}$ is an externally applied magnetic field. It was first discovered by Edwin Hall in 1879, eighteen years before the discovery of the electron, and originally dubbed as "a new action of the magnet on electric currents" [11].

We take our setup to be as in Figure 5. An electric field $\mathbf{E} = E_x\hat{\mathbf{x}}$ is applied to a wire lying along the x-axis, inducing a charge current $\mathbf{j} = j_x\hat{\mathbf{x}}$ through the wire. In addition we apply a magnetic field $\mathbf{B} = B_z\hat{\mathbf{z}}$. Due to the presence of this magnetic field, the electrons will be acted upon by the Lorentz force

$$\mathbf{F}_L = -\frac{e}{c}\mathbf{v} \times \mathbf{B}\,, \tag{2.5}$$

effectively deflecting the electrons in the negative y-direction (note that the velocity $\mathbf{v}$ of an electron is in the opposite direction of the charge current $\mathbf{j}$). However, the electrons can not keep moving in this direction forever since at a certain point they will have reached the boundary of the conductor. At this boundary, the negatively charged electrons accumulate. There they induce an electric field along the y-axis, opposite to the direction of flow of the charge. The opposing electric field impedes further accumulation of charge until an equilibrium is attained. The transverse field E_y, known as the Hall field, balances the Lorentz force. Because of this, the charge current will eventually be only along the x-axis (see Figures 5b and 5c).

Using the Drude model, we can determine the size of the Hall field. Since this field balances the Lorentz force, we expect it to be proportional to the external magnetic field and to the current along the wire. This motivates us to define the Hall coefficient

Figure 5: the (classical) Hall effect. In (a) we have the geometry of our setup. In (b) we see that the electrons are deflected in the negative y-direction. In (c) we have reached a steady state. Reprinted from Reference [12].

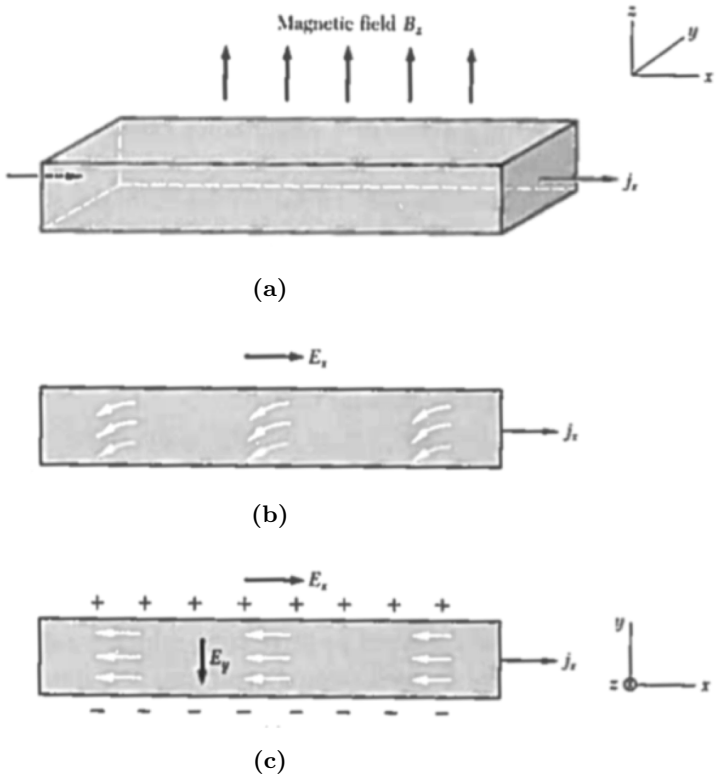

$$R_H = \frac{E_y}{j_x B}\,. \tag{2.6}$$

To calculate the Hall coefficient, we must first find the equation of motion for an electron in Hall's experiment. We do so by adding to $\mathbf{F}$ in (2.1) the Lorentz force $\mathbf{F}_L$ (2.5) so that $\mathbf{F} = \mathbf{F}_{el} + \mathbf{F}_L$ yielding

$$\dot{\mathbf{p}} = -e\Big(\mathbf{E} + \frac{\mathbf{p}}{mc} \times \mathbf{B}\Big) - \frac{\mathbf{p}}{\tau}\,.$$

By considering the steady state once more, we find that we must satisfy

$$\begin{aligned} -eE_x - \frac{eB}{mc}p_y - \frac{p_x}{\tau} &= 0\,, \\ -eE_y - \frac{eB}{mc}p_x - \frac{p_y}{\tau} &= 0\,. \end{aligned}$$

Multiplying both equations by $-ne\tau/m$ and using (2.3) we get

$$\sigma E_x = \frac{eB\tau}{mc} j_y + j_x \,, \tag{2.7}$$

$$\sigma E_y = -\frac{eB\tau}{mc} j_x + j_y \,, \tag{2.8}$$

where σ is just the Drude model DC electrical conductivity given in (2.4). For the Hall field E_y we must have that $j_y = 0$ (we argued that eventually there would be no charge current other than along the x-axis). Setting the transverse current to zero in the equations (2.7) and (2.8) we find

$$\begin{aligned} E_x &= \frac{1}{\sigma} j_x \,, \\ E_y &= -\frac{eB\tau}{\sigma mc} j_x = -\frac{B}{nec} j_x \,. \end{aligned} \tag{2.9}$$

Note that the first of these equations is simply what we found before in (2.4), without the presence of a magnetic field **B**. This implies that the transverse magnetoresistance

$$\rho = \frac{E_x}{j_x} \,,$$

defined as the inverse of the conductivity, is independent of the magnetic field (and hence so is the conductivity σ itself). From (2.9) we find that the Hall coefficient (2.6) must be

$$R_H = -\frac{1}{nec} \,.$$

This is a remarkable result, because it states that the Hall coefficient depends only on the density of the charge carriers in the metal. For a given metal then (which can be calculated to have some fixed density of charge carriers), the Hall coefficient is a constant; it is independent of the temperature, the relaxation time and the strength of the magnetic field. From experiments though, we know that the Hall coefficient does depend on these quantities. This inadequate description stems from the assumptions we made constructing the Drude model. In Subsection 2.2, we drop the free electron approximation and look at what happens when we include the spin-orbit interactions of the electrons.

2.2 Spin Hall effect

In this Subsection we extend the Drude model to account for the spin-orbit interactions of the electrons, eliciting the spin Hall effect. The effect was first predicted by the Russian physicists Mikhail Dyakonov and Vladimir Perel in 1971 [13]. Qualitatively, the spin Hall effect can be understood through an analogy with the classical Hall effect. Just as a transverse charge current would flow in the classical Hall setup as a result of an external magnetic field (Figure 5), a transverse spin current starts to flow as a result of an

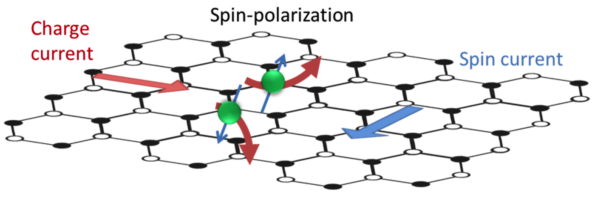

Figure 6: the spin Hall effect. Induced by a charge current, a transverse spin current starts to flow. Copyright: https://en.wikipedia.org/wiki/Spin-Hall-effect.

external electric field due to the spin Hall effect (Figure 6). Note that for the spin Hall effect, we require the presence of an external electric field only (i.e. no external magnetic field is needed).

In an approach similar to uncovering an expression for the charge conductivity σ in (2.4), we will find one for the spin Hall conductivity σ_{SH}. For the sake of including the spin-orbit interaction, we have to perform Hamiltonian mechanics on the non-relativistic limit of the Dirac Hamiltonian for a spin-1/2 particle which looks like

$$H = \frac{\mathbf{p}^2}{2m} + U(\mathbf{r}) + \frac{\hbar}{4m^2c^2}\boldsymbol{\sigma} \cdot \left[\frac{\partial U}{\partial \mathbf{r}} \times \mathbf{p}\right].$$

Here the last term is the spin-orbit interaction, with $\boldsymbol{\sigma}$ being Pauli matrices. Furthermore $U(\mathbf{r})$ incorporates the effects on charge carriers of the electrostatic crystal potential Φ_0, the potential due to imperfections in the crystal lattice Φ_i and the external potential Φ_e so that $U(\mathbf{r}) = e\Phi_0(\mathbf{r}) + e\Phi_i(\mathbf{r}) + e\Phi_e(\mathbf{r})$. We then find for the canonically conjugated variables $\mathbf{r}$ and $\mathbf{p}$ that

$$\dot{\mathbf{r}} = \frac{\mathbf{p}}{m} + \frac{\hbar}{4m^2c^2}\left[\boldsymbol{\sigma} \times \frac{\partial U}{\partial \mathbf{r}}\right], \tag{2.10}$$

$$\dot{\mathbf{p}} = -\frac{\partial U}{\partial \mathbf{r}} - \frac{\hbar}{4m^2c^2}\frac{\partial}{\partial \mathbf{r}}\left(\left[\boldsymbol{\sigma} \times \frac{\partial U}{\partial \mathbf{r}}\right] \cdot \mathbf{p}\right). \tag{2.11}$$

From (2.10) we get

$$\mathbf{p} = m\dot{\mathbf{r}} - \frac{\hbar}{4mc^2}\left[\boldsymbol{\sigma} \times \frac{\partial U}{\partial \mathbf{r}}\right], \tag{2.12}$$

$$\dot{\mathbf{p}} = m\ddot{\mathbf{r}} - \frac{\hbar}{4mc^2}\left(\dot{\mathbf{r}} \cdot \frac{\partial}{\partial \mathbf{r}}\right)\left[\boldsymbol{\sigma} \times \frac{\partial U}{\partial \mathbf{r}}\right]. \tag{2.13}$$

Substituting equations (2.12) and (2.13) into (2.11) yields the following version of Newton's second law of motion for the electrons

$$m\ddot{\mathbf{r}} = -\frac{\partial U}{\partial \mathbf{r}} + \mathbf{F}_{\boldsymbol{\sigma}}(\mathbf{r}, \dot{\mathbf{r}}), \tag{2.14}$$

where the spin-dependent force is given by

$$\begin{aligned}\mathbf{F}_{\boldsymbol{\sigma}}(\mathbf{r}, \dot{\mathbf{r}}) &= \frac{\hbar}{4mc^2}\left\{\left(\dot{\mathbf{r}} \cdot \frac{\partial}{\partial \mathbf{r}}\right)\left[\boldsymbol{\sigma} \times \frac{\partial U}{\partial \mathbf{r}}\right] - \frac{\partial}{\partial \mathbf{r}}\left(\dot{\mathbf{r}} \cdot \left[\boldsymbol{\sigma} \times \frac{\partial U}{\partial \mathbf{r}}\right]\right)\right\} \\ &= -\frac{\hbar}{4mc^2}\dot{\mathbf{r}} \times \left[\frac{\partial}{\partial \mathbf{r}} \times \left(\boldsymbol{\sigma} \times \frac{\partial U}{\partial \mathbf{r}}\right)\right].\end{aligned} \tag{2.15}$$

We remark that the term proportional to $1/c^4$ has been neglected. One should note that the spin-dependent force (2.15) is equivalent to a Lorentz force $\mathbf{F}_{\boldsymbol{\sigma}} = (-e/c)(\dot{\mathbf{r}} \times \mathbf{B}_{\boldsymbol{\sigma}})$ acting on an electron in the magnetic field

$$\mathbf{B}_{\boldsymbol{\sigma}} = \boldsymbol{\nabla} \times \mathbf{A}_{\boldsymbol{\sigma}} \text{ with } \mathbf{A}_{\boldsymbol{\sigma}} = \frac{\hbar}{4mc}(\boldsymbol{\sigma} \times \mathbf{E}_{tot}),$$

where $\mathbf{E}_{tot}$ is the total electric field given by $-\partial U/\partial \mathbf{r} = (-e)\mathbf{E}_{tot}$. Hence (2.14) reads $m\ddot{\mathbf{r}} = -e\mathbf{E}_{tot} + \mathbf{F}_{\boldsymbol{\sigma}}$. The force $\mathbf{F}_{\boldsymbol{\sigma}}$ thus is an effective Lorentz force, dependent on the spin polarization, leading to the spin Hall effect. Now to find the spin Hall conductivity we add, in the spirit of the Drude model, the frictional damping term $-m\dot{\mathbf{r}}/\tau$ to the law of motion (2.14) so that we get

$$m\ddot{\mathbf{r}} = -e\mathbf{E}_{tot} + \mathbf{F}_{\boldsymbol{\sigma}} - \frac{m\dot{\mathbf{r}}}{\tau}\,.$$

From this it can be shown that under the assumption of a cubic lattice [10]

$$\mathbf{j} = \sigma\mathbf{E} + \sigma_{SH}\big(\boldsymbol{\xi} \times \mathbf{E}\big) \text{ where } \sigma = \frac{ne^2\tau}{m} \text{ as before and } \sigma_{SH} = \frac{\hbar n e^3 \tau^2 A}{2m^3c^2}\,. \tag{2.16}$$

Here $\mathbf{E} = -\partial\Phi_e/\partial\mathbf{r}$ denotes the constant external electric field and $\boldsymbol{\xi}$ denotes the spin polarization of the electrons. The spin polarization has magnitude $\xi = (n_+ - n_-)/(n_+ + n_-)$ where n_+ and n_- are the concentrations of electrons with spins parallel and antiparallel to $\boldsymbol{\xi}$ respectively (so that $n = n_+ + n_-$ is the total concentration of electrons). In addition we have that A, which is the volume average of a second derivative of a potential contribution, reduces to some constant in the case of a cubic lattice. We have now derived an expression for the spin Hall conductivity σ_{SH}. Normally we would write $\sigma_{SH} = \sigma\theta$, introducing the spin Hall angle θ which is usually small. From (2.16) we find under the assumptions we have made throughout that

$$\theta = \frac{\hbar e \tau A}{2m^2c^2}\,.$$

For us the most important part of this Subsection is the appearance of a spin-dependent force, equivalent to the Lorentz force, acting on the electrons. It reveals the spin Hall effect as a consequence of spin-orbit interactions. Just as charge accumulates on the boundaries of a metal due to the (classical) Hall effect, so does a generic charge current prompt a spin accumulation in the metal due to the spin Hall effect. The implications of this spin accumulation become apparent in Section 4 in which we consider a bilayer of a nonmagnetic metal and a ferromagnetic insulator. In Section 3 however, we first discuss ferromagnets.

3 Ferromagnets

In this Section we discuss the ferromagnetic configuration of a lattice of electron spins and see how magnons arise. As a model of a ferromagnet, consider a set of electron spins at Bravais lattice sites $\mathbf{R}$. The Bravais lattice under consideration we take to be a hypercubic one of dimension d with lattice spacing a and with N sites. Also we suppose that the lattice is subjected to Born-von Karman periodic boundary conditions. We assume the spins interact with only their nearest neighbours. Furthermore, we do not place our ferromagnet in an external field. This system then is described by the Hamiltonian

$$H = -\frac{J}{2} \sum_{\mathbf{R}\mathbf{R}'} \mathbf{S}(\mathbf{R}) \cdot \mathbf{S}(\mathbf{R}') \,, \tag{3.1}$$

where we take the exchange interaction J to be positive since this favours parallel spin alignment (and hence gives the correct Hamiltonian for a ferromagnet). In the case of a hypercubic lattice, the exchange interaction is a constant and can therefore be taken out of the summand. Additionally $\mathbf{S}(\mathbf{R})$ represents the spin at lattice site $\mathbf{R}$. The nearest neighbours of the spin at site $\mathbf{R}$ are indicated by $\mathbf{R}'$ and so the sum indicates that for all the sites we evaluate the interactions with all the nearest neighbours. The factor of one half then appears, because by summing over all the nearest neighbours of all the spins we have actually examined each pair interaction twice.

In Subsection 3.1, which is largely based on Reference [14], we give a semi-classical treatment of the Hamiltonian (3.1) as we regard the spins $\mathbf{S}(\mathbf{R})$ as classical vectors. After this we treat our Hamiltonian quantum mechanically in Subsection 3.2, which follows Reference [9], and consider the spins to be operators.

3.1 Semi-classical treatment of Hamiltonian

We initially take our ferromagnet to be in its ground state. That is to say that all the spins point in the same direction. Let us assume they do so in the positive z-direction. Our aim is to find the equation of motion for a spin at a given lattice site. From the Ehrenfest theorem, we derive the following equation of motion for $\mathbf{S}(\mathbf{R})$:

$$\dot{\mathbf{S}}(\mathbf{R}) = -\mathbf{S}(\mathbf{R}) \times \frac{\partial H}{\partial \mathbf{S}(\mathbf{R})} \,. \tag{3.2}$$

The partial derivative of the Hamiltonian evaluates to $-J \sum_{\mathbf{R}'} \mathbf{S}(\mathbf{R}')$. On the other hand, since we took our ferromagnet to be in its ground state and therefore all the spins are static, the time derivative of the spin on the left-hand side of (3.2) is zero (as is the cross product on the right-hand side of the spin with the partial derivative of the Hamiltonian). Therefore nothing of interest is happening in the ground state. To get low-energy excitations out of this ground state, we slightly nudge our spin out of its equilibrium position:

$$\mathbf{S}(\mathbf{R}) = \begin{bmatrix} \delta S_x(\mathbf{R}) \\ \delta S_y(\mathbf{R}) \\ \hbar S \end{bmatrix} \,,$$

where $\delta S_x(\mathbf{R})$ and $\delta S_y(\mathbf{R})$ are small and time-dependent and where $\hbar S$ is the ground state magnitude of the spin with $\hbar$ being Planck's constant divided by 2π (note that for an electron $S = 1/2$). Substituting this expression into the equation of motion (3.2), we find that

$$\dot{\delta S}_x(\mathbf{R}) = J\hbar S\Big(2\delta S_y(\mathbf{R}) - \sum_{\mathbf{R}'} \delta S_y(\mathbf{R}')\Big)\,, \tag{3.3}$$

$$\dot{\delta S}_y(\mathbf{R}) = -J\hbar S\Big(2\delta S_x(\mathbf{R}) - \sum_{\mathbf{R}'} \delta S_x(\mathbf{R}')\Big)\,, \tag{3.4}$$

where the equation for the z-component has been omitted since both sides of (3.2) yield a zero value for this component. (Obviously, the time derivative is zero because the z-component is constant in time. The cross product vanishes because it is second order in the small deviations, allowing us to withhold these terms.) In order to solve these equations and expecting a spin wave, we make the plane-wave ansatz

$$\begin{bmatrix}\delta S_x(\mathbf{R})\\ \delta S_y(\mathbf{R})\end{bmatrix} = \begin{bmatrix}\epsilon_x\\ \epsilon_y\end{bmatrix} e^{i(\mathbf{k}\cdot\mathbf{R}-\omega t)}\,, \tag{3.5}$$

where ϵ_x and ϵ_y are (small) amplitudes, $\mathbf{k}$ is the wave vector and ω is the frequency. Substituting this into the equations (3.3) and (3.4) gives us that

$$\begin{bmatrix} i\omega & J\hbar S\big(2 - \sum_{\mathbf{R}'} e^{i\mathbf{k}\cdot(\mathbf{R}'-\mathbf{R})}\big)\\ -J\hbar S\big(2 - \sum_{\mathbf{R}'} e^{i\mathbf{k}\cdot(\mathbf{R}'-\mathbf{R})}\big) & i\omega\end{bmatrix}\begin{bmatrix}\epsilon_x\\ \epsilon_y\end{bmatrix} = \mathbf{0}\,, \tag{3.6}$$

where in the process we divided by $\exp[i(\mathbf{k}\cdot\mathbf{R} - \omega t)]$. Solving this eigenvalue problem for the frequency (by setting the determinant of the matrix equal to zero) we would find the dispersion relation $\omega_{\mathbf{k}}$. For simplicity though, let us first assume that our lattice is one-dimensional. In the one-dimensional case, we have $\mathbf{k} = k$ and $\mathbf{R} = na$ where n is of integral value (i.e. including zero and the negatives). Also note that in one dimension every spin has two nearest neighbours (at positions $(n-1)a$ and $(n+1)a$ for a spin at position na). Substituting this into the matrix of (3.6) and solving for the frequency then yields the dispersion relation

$$\omega_k = 4J\hbar S \sin^2(ka/2)\,,$$

where we have sufficed in taking only the positive root. We have plotted the frequency against the wave vector in Figure 7. From this dispersion relation, we can determine the ratio of the amplitudes

$$\frac{\epsilon_x}{\epsilon_y} = i\,.$$

Note that the other (trivial) eigenvector ($\epsilon_x = \epsilon_y = 0$) corresponds to the static solution. Using $\epsilon_x/\epsilon_y = i$ (and by taking the real part of the solution) we get from the plane-wave ansatz (3.5)

$$\begin{bmatrix}\delta S_x(\mathbf{R})\\ \delta S_y(\mathbf{R})\end{bmatrix} \propto \begin{bmatrix}-\sin(kna - \omega_k t)\\ \cos(kna - \omega_k t)\end{bmatrix}\,. \tag{3.7}$$

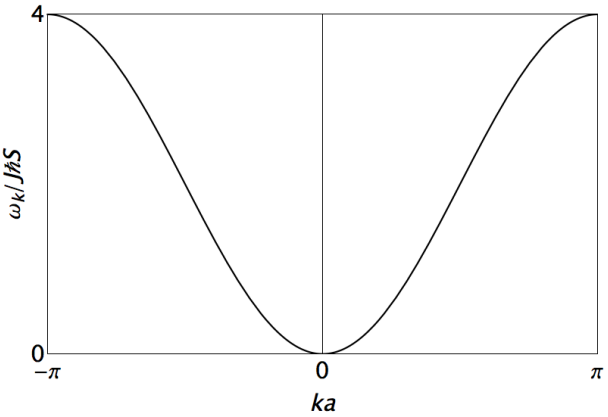

Figure 7: dispersion curve for a spin wave through a one-dimensional ferromagnetic lattice with only nearest neighbour interactions.

We have now found our spin wave. The solution (3.7) can be imagined to be a spin precessing clockwise (viewed from above) around the unit vector $\hat{\mathbf{z}}$, as in Figure 2b, with a frequency of ω_k. The term kna then denotes a phase shift, where each spin is rotated by ka with respect to the previous spin.

3.2 Quantum mechanical treatment of Hamiltonian

In a quantum mechanical approach, we have to regard the spins as operators $\hat{\mathbf{S}}(\mathbf{R})$. Again we begin by putting our ferromagnet in its ground state. All the spins then point in the same direction, which we assume to be the positive z-direction. Because of this, a candidate for the quantum mechanical ground state $|0\rangle$ is one that is an eigenstate of $\hat{S}_z(\mathbf{R})$ for all $\mathbf{R}$ and with the eigenvalue S. Mathematically, this reduces to

$$|0\rangle = \prod_{\mathbf{R}} |S\rangle_{\mathbf{R}} \text{ where } \hat{S}_z(\mathbf{R})\,|S\rangle_{\mathbf{R}} = S\,|S\rangle_{\mathbf{R}}\ . \tag{3.8}$$

To show that $|0\rangle$ indeed denotes the ground state, we must first verify that it is in fact an eigenstate of the Hamiltonian (3.1). In order to do so, we rewrite the Hamiltonian in terms of the operators

$$\hat{S}_{\pm}(\mathbf{R}) = \hat{S}_x(\mathbf{R}) \pm i\hat{S}_y(\mathbf{R})\,,$$

possessing the property

$$\hat{S}_{\pm}(\mathbf{R})\,|S_z\rangle_{\mathbf{R}} = \sqrt{(S \mp S_z)(S+1 \pm S_z)}\,|S_z \pm 1\rangle_{\mathbf{R}}\ . \tag{3.9}$$

This allows us to write the Hamiltonian as

$$\hat{H} = -\frac{J}{2}\sum_{\mathbf{RR'}} \Big(\hat{S}_z(\mathbf{R})\hat{S}_z(\mathbf{R}') + \hat{S}_-(\mathbf{R}')\hat{S}_+(\mathbf{R})\Big)\,. \tag{3.10}$$

Now by virtue of (3.9) we have $\hat{S}_+(\mathbf{R})\,|S_z\rangle_{\mathbf{R}} = 0$ when $S_z = S$ (which corresponds to the ground state of the ferromagnet). That is, we can not raise the z-component of a spin any further when this component already assumes its maximum value. Hence the only terms that contribute when $\hat{H}$ acts on the ground state $|0\rangle$, are the ones involving the operators $\hat{S}_z$. Since $|0\rangle$ is constructed to be an eigenstate of each of the operators $\hat{S}_z(\mathbf{R})$ with eigenvalue S, this yields

$$\hat{H}\,|0\rangle = E_0\,|0\rangle \text{ with } E_0 = -NdJS^2\,.$$

We see that $|0\rangle$ is indeed an eigenstate of $\hat{H}$ and have found its accompanying eigenvalue E_0. It can be proved that E_0 is in fact the *ground* state energy of the system (i.e. there does not exist $E_0' < E_0$ where $\hat{H}\,|0\rangle = E_0'\,|0\rangle$) [9]. In conclusion then, the quantum mechanichal ground state of the ferromagnet is given by $|0\rangle$ as defined in (3.8).

Having found this ground state, we will now look for low-lying excited states of the Hamiltonian that appear whenever we have a nonzero temperature. We first examine a state $|\mathbf{R}\rangle$ in which we have flipped from the ground state $|0\rangle$, where all the spins would align, the electron spin at position $\mathbf{R}$. This should remind us of the type of excitation which we hand-wavingly argued to be insufficient in Section 1. We will indeed see that $|\mathbf{R}\rangle$ is not an eigenstate of the ferromagnetic Hamiltonian. Nonetheless, we will be able to find linear combinations of $|\mathbf{R}\rangle$ that are eigenstates and which turn out to be the magnons we are looking for. Mathematically, the state $|\mathbf{R}\rangle$ (normalized to unity) looks as follows

$$|\mathbf{R}\rangle = \frac{1}{\sqrt{2S}}\hat{S}_-(\mathbf{R})\,|0\rangle\ ,$$

where we have thus reduced the z-component of the spin particle at $\mathbf{R}$ from S to $S-1$. For $S=1/2$ this is equivalent to flipping the spin at site $\mathbf{R}$. If we were to put $|\mathbf{R}\rangle$ back into the Hamiltonian operator (3.10), we would see that $|\mathbf{R}\rangle$ remains an eigenstate of the terms involving the operators $\hat{S}_z(\mathbf{R})$. However, because now the spin at $\mathbf{R}$ does not assume its maximum z-component (since we have actively lowered this by one), $\hat{S}_+(\mathbf{R})\,|\mathbf{R}\rangle$ will not vanish. Moreover, by letting $\hat{S}_-(\mathbf{R}')\hat{S}_+(\mathbf{R})$ act on $|\mathbf{R}\rangle$ we first add one to the z-component of the spin we just lowered by one and then lower the spin of one of the nearest neighbours by one. We find

$$\hat{S}_-(\mathbf{R}')\hat{S}_+(\mathbf{R})\,|\mathbf{R}\rangle = 2S\,\big|\mathbf{R}'\big\rangle\ .$$

Additionally we have that

$$\hat{S}_z(\mathbf{R}')\,|\mathbf{R}\rangle = S\,|\mathbf{R}\rangle\ ,$$

since measuring the z-component of any spin from the state $|\mathbf{R}\rangle$ that has not been flipped simply yields the maximum value S. (We know that we do not measure the flipped spin at $\mathbf{R}$ because $\mathbf{R}'$ is defined to be a nearest neighbour of $\mathbf{R}$.) It follows that

$$\hat{H}\,|\mathbf{R}\rangle = E_0\,|\mathbf{R}\rangle + JS\sum_{\mathbf{R}'}\big(\,|\mathbf{R}\rangle - \big|\mathbf{R}'\big\rangle\,\big)\,. \tag{3.11}$$

As predicted, $|\mathbf{R}\rangle$ is not an eigenstate of the Hamiltonian but we see that $\hat{H}\,|\mathbf{R}\rangle$ does turn out to be a linear combination of $|\mathbf{R}\rangle$ and other states that have only a single lowered spin. From these we can construct the linear combination

$$|\mathbf{k}\rangle = \frac{1}{\sqrt{N}}\sum_{\mathbf{R}} e^{i\mathbf{k}\cdot\mathbf{R}}\,|\mathbf{R}\rangle\ ,$$

which does form an eigenstate. From (3.11) we infer

$$\hat{H}\,|\mathbf{k}\rangle = E_{\mathbf{k}}\,|\mathbf{k}\rangle \text{ with } E_{\mathbf{k}} = E_0 + JS\sum_{\mathbf{R}}\left(1 - e^{i\mathbf{k}\cdot\mathbf{R}}\right).$$

The expression for the eigenvalue allows us to write the excitation energy $\mathcal{E}_{\mathbf{k}}$ of the state $|\mathbf{k}\rangle$, i.e. the energy that is extra in comparison with the energy from the ground state, as

$$\mathcal{E}_{\mathbf{k}} = E_{\mathbf{k}} - E_0 = 2JS\sum_{\mathbf{R}}\sin^2\left(\frac{\mathbf{k}\cdot\mathbf{R}}{2}\right). \tag{3.12}$$

We see that if there is no wave (i.e. $\mathbf{k} = \mathbf{0}$, a wave with infinite wavelength) then the excitation energy is zero, reducing this case to the ground state (i.e. $|\mathbf{0}\rangle = |0\rangle$). For a physical interpretation of the state $|\mathbf{k}\rangle$ whenever $\mathbf{k} \neq \mathbf{0}$ we make some observations.

As noted before, the state $|\mathbf{k}\rangle$ is a superposition of states in which each of those states has had its total possible spin of SN reduced by one. That is to say that the total spin of the state $|\mathbf{k}\rangle$ is equal to $SN - 1$. Secondly we remark that the probability of the lowered spin being found at a certain lattice site $\mathbf{R}$ in the state $|\mathbf{k}\rangle$ is $|\langle \mathbf{k}|\mathbf{R}\rangle|^2 = 1/N$. This means that the lowered spin is distributed with equal probability among all the spin lattice sites. Lastly, we define the transverse spin correlation function in the state $|\mathbf{k}\rangle$ to be the expectation value of

$$\hat{\mathbf{S}}_\perp(\mathbf{R}) \cdot \hat{\mathbf{S}}_\perp(\mathbf{R}') = \begin{bmatrix} \hat{S}_x(\mathbf{R}) \\ \hat{S}_y(\mathbf{R}) \end{bmatrix} \cdot \begin{bmatrix} \hat{S}_x(\mathbf{R}') \\ \hat{S}_y(\mathbf{R}') \end{bmatrix} ,$$

which turns out to be

$$\langle \mathbf{k}| \, \hat{\mathbf{S}}_\perp(\mathbf{R}) \cdot \hat{\mathbf{S}}_\perp(\mathbf{R}') \, |\mathbf{k}\rangle = \frac{2S}{N} \cos\big(\mathbf{k} \cdot (\mathbf{R} - \mathbf{R}')\big) \text{ whenever } \mathbf{R} \neq \mathbf{R}' .$$

We interpret this result along the following lines. On average each spin turns out to have a small transverse component, perpendicular to the direction of the magnetization, of magnitude $\sqrt{2S/N}$. The directions of the transverse components of two spins separated by $\mathbf{R} - \mathbf{R}'$ differ by an angle $\mathbf{k} \cdot (\mathbf{R} - \mathbf{R}')$. For a one-dimensional lattice one would picture this state $|\mathbf{k}\rangle$ like Figure 2b. The state $|\mathbf{k}\rangle$ is described as containing a magnon of wave vector $\mathbf{k}$ and of energy $\mathcal{E}_\mathbf{k}$ as given in (3.12).

4 Bilayers

In Sections 2 and 3 respectively, we have quantitatively seen how spin-orbit interactions of the valence electrons in a nonmagnetic metal lead to the spin Hall effect and how magnons arise as the low-lying excited states of a ferromagnet. In this Section we examine what happens when we have a bilayer of a nonmagnetic metal and a ferromagnetic insulator (also frequently denoted as NM/FM bilayer). We do so in a more qualitative way. Let us first define the geometry of our setup.

The bilayer under consideration has a ferromagnetic insulator placed on top of a nonmagnetic metal. The average spin direction in the ferromagnet is taken to be static and in alignment with the unit vector $\hat{\mathbf{n}}$. The interface between the two layers is taken to be normal to the z-axis. We let the charge current $\mathbf{j}_c$ flow along the interface in the positive x-direction (hence the external electric field is also in this direction). The spin accumulation induced by the spin Hall effect then has its spin polarization in the y-direction. See Figure 8 for a picture of this setup.

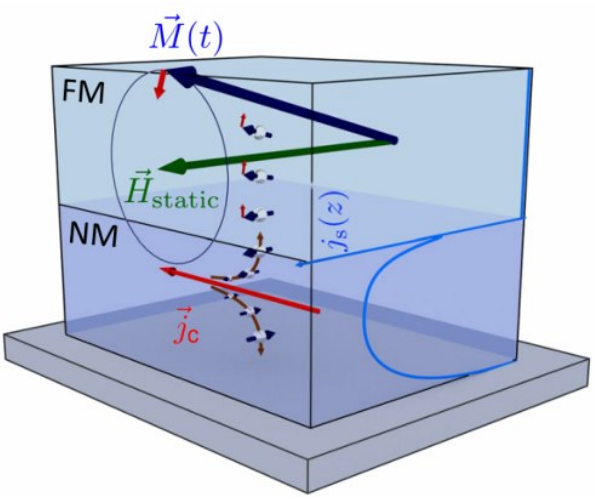

Figure 8: geometry of our setup of a NM/FM bilayer. Here we took the direction of the average spin in the ferromagnet to be in the positive y-direction i.e. $\hat{\mathbf{n}} = \hat{\mathbf{y}}$. Copyright: http://www.uni-regensburg.de/physik/back/research/index.html.

Before concerning ourselves with effects due to the combination of a nonmagnet and a ferromagnet in Subsection 4.3, we first state without rigorous derivation some equations that hold in nonmagnets (Subsection 4.1) and ferromagnets (Subsection 4.2) separately. In this Section we simply state the appropriate spin transport equations. In Section 5 we apply these equations to the USMR.

4.1 Nonmagnetic metal

In the nonmagnetic metal, the charge current and the electron spin current (brought about by the freely moving electrons) are given by [15]

$$\begin{aligned} j_c &= \sigma E + \frac{\sigma\theta}{2e}\frac{\partial \mu_s}{\partial z}\,, \\ \frac{2e}{\hbar} j_s^e &= -\frac{\sigma}{2e}\frac{\partial \mu_s}{\partial z} - \sigma\theta E\,, \end{aligned}$$

where the electric field $\mathbf{E}$ and the charge current $\mathbf{j}_c$ are along the x-direction. The spin accumulation μ_s in the nonmagnetic metal is along the y-direction so that the spin current j_s has spin polarization along the y-direction as well and flows along the z-direction. We also have the familiar DC electrical conductivity σ, Planck's constant divided by 2π denoted as $\hbar$, the electron charge e and the spin Hall angle θ which is assumed to be small. In addition, the spin diffusion equation in the metal is given by [15]

$$\frac{\partial^2 \mu_s}{\partial z^2} = \frac{\mu_s}{\ell_s^2}\,,$$

where ℓ_s is the spin relaxation length of the nonmagnetic metal. Again we note that we have considered the spin accumulation to be in the y-direction.

4.2 Ferromagnet

In the ferromagnet the magnon spin current (brought about by the spin waves) is given by [15]

$$j_s^m = -\frac{\sigma_m}{\hbar}\frac{\partial \mu_m}{\partial z}\,,$$

where σ_m is the magnon spin conductivity and μ_m is the magnon spin accumulation. Additionally we have a diffusion equation, this time for the magnons, which is given by [15]

$$\frac{\partial^2 \mu_m}{\partial z^2} = \frac{\mu_m}{\ell_m^2}\,,$$

where ℓ_m is the magnon spin relaxation length.

4.3 Interfacial spin current

Having given expressions for the electron spin current j_s^e in the nonmagnetic metal and the magnon spin current j_s^m in the ferromagnetic insulator, we now take a look at the interfacial spin current. This current arises across the interface between the two layers as a result of the coupling interaction between the electron spin in the nonmagnetic metal and the magnon spin in the ferromagnetic insulator. For the interfacial spin current we have [16]

$$\mathbf{j}_s^{int} = \frac{g_r^{\uparrow\downarrow}}{4\pi}\hat{\mathbf{n}} \times (\mu_s \hat{\mathbf{y}} \times \hat{\mathbf{n}}) + g_s(\mu_m + \hat{\mathbf{n}} \cdot \hat{\mathbf{y}})\hat{\mathbf{n}}\,, \tag{4.1}$$

where thermal corrections to the spin transfer torques have been neglected. Here $g_r^{\uparrow\downarrow}$ is the real part of the interface spin mixing conductance (where its imaginary part has been neglected) and g_s denotes the spin conductance for longitudinal spin (i.e. spin transport with polarization along $\hat{\mathbf{n}}$) which is given by

$$g_s = \frac{3\zeta(3/2)g_r^{\uparrow\downarrow}}{2\pi s \Lambda_m^3}\,,$$

where $\zeta(x)$ is the Riemann zeta function, s the equilibrium spin density in the ferromagnet and where the thermal de Broglie wavelength for the magnons is given by

$$\Lambda_m = \sqrt{\frac{4\pi J_s}{k_B T_m}}\,.$$

Here J_s denotes the exchange stifness of the ferromagnet and T_m is the temperature of the ferromagnet. We ignore the transverse spin current i.e. the first term in (4.1). This would give rise to the conventional spin

Hall magnetoresistance which is of no interest to us here. Taking the direction of the average spin in the ferromagnet to be in the positive y-direction i.e. setting $\hat{\mathbf{n}} = \hat{\mathbf{y}}$, we are able to write the interfacial spin current (4.1) as [16]

$$j_s^{int} = -\frac{g_r^{\uparrow\downarrow}}{\pi s}\int_0^\infty d\epsilon D(\epsilon)(\epsilon-\mu_s)\left[n\left(\frac{\epsilon-\mu_m}{k_BT_m}\right)-n\left(\frac{\epsilon-\mu_s}{k_BT_e}\right)\right], \tag{4.2}$$

where $D(\epsilon)$ denotes the magnon density of states and $n(x) = (e^x-1)^{-1}$ is the Bose-Einstein distribution function. We assume that the interfacial spin current can be described as the sum of two independent parts. One of those will vary only on the accumulations μ_s and μ_m and the other only on the temperature of the metal T_e and the temperature of the magnet T_m:

$$j_s^{int} = j_{s,\mu}^{int} + j_{s,T}^{int}\,.$$

Before we continue, a word on the magnon density of states introduced in (4.2). In Section 3 we expressed the Hamiltonian (3.1) from which we found the magnon energy (3.12). Up to and including first nontrivial order in the wave vector, we can write the magnon energy as $\mathcal{E}_{\mathbf{k}} = \alpha k^2$ where α is some proportionality constant. The magnon density of states can then be calculated to be $D(\epsilon) = \sqrt{\epsilon}/4\pi^2 J_s^{3/2}$, where $\sqrt{\epsilon}$ appears as the radius of the sphere in momentum space enclosing all possible states up to a certain energy.

To be complete, we will give expressions for the temperature dependent and the accumulation dependent part of the interfacial spin current. However, when we compute the magnon contribution to the unidirectional spin Hall magnetoresistance in Section 5, we only take into account the accumulation dependent part. In other words, we will assume that the temperature of the nonmagnetic metal and that of the ferromagnetic insulator are equal (an assumption that is false because of the different thermal properties of the two materials). By doing so, the temperature dependent part of the interfacial spin current vanishes.

4.3.1 Temperature dependent part

We first compute the term depending on the difference in temperature $\Delta T = T_e - T_m$ only. By setting $\mu_s = \mu_m = 0$ we find for the temperature dependent part of the interfacial spin current (4.2) that

$$j_{s,T}^{int} = -\frac{g_r^{\uparrow\downarrow}}{\pi s}\int_0^\infty d\epsilon D(\epsilon)\epsilon\left[n\left(\frac{\epsilon}{k_B(T_e-\Delta T)}\right)-n\left(\frac{\epsilon}{k_BT_e}\right)\right]. \tag{4.3}$$

Taylor expanding the expression in square brackets of (4.3) up to and including first order as in Appendix A.1 and substituting this into (4.3), we find using Appendix A.3

$$\begin{aligned} j_{s,T}^{int} &= -\frac{g_r^{\uparrow\downarrow}}{\pi s}\int_0^\infty d\epsilon D(\epsilon)\epsilon\left[\frac{\epsilon}{T_e}\frac{\partial}{\partial\epsilon}\left(e^{\epsilon/k_BT_e}-1\right)^{-1}\right]\Delta T + \mathcal{O}\big[(\Delta T)^2\big] \\ &= \frac{3g_r^{\uparrow\downarrow}\zeta(5/2)}{2\pi s\Lambda_e^3}\frac{5k_B}{2}\Delta T + \mathcal{O}\big[(\Delta T)^2\big]\,. \end{aligned}$$

Here $\Lambda_e = \sqrt{4\pi J_s/k_BT_e}$ is the thermal de Broglie wavelength for electrons and we took the magnon density of states to be $D(\epsilon) = \sqrt{\epsilon}/4\pi^2 J_s^{3/2}$.

4.3.2 Accumulation dependent part

For the accumulation dependent part of the interfacial spin current we set $T = T_e = T_m$ (so $\Lambda = \Lambda_e = \Lambda_m$) in (4.2) and let $\beta = 1/k_B T$ so that

$$j_{s,\mu}^{int} = -\frac{g_r^{\uparrow\downarrow}}{\pi s}\int_0^\infty d\epsilon D(\epsilon)(\epsilon-\mu_s)\big[n\big(\beta(\epsilon-\mu_m)\big) - n\big(\beta(\epsilon-\mu_s)\big)\big]\,. \tag{4.4}$$

By a Taylor expansion up to and including second order of the expression in square brackets of (4.4) as in Appendix A.2 and by substituting this into (4.4), we find

$$\begin{aligned} j_{s,\mu}^{int} =& -\frac{g_r^{\uparrow\downarrow}}{\pi s}\int_0^\infty d\epsilon D(\epsilon)(\epsilon-\mu_s)\bigg[-\frac{\partial}{\partial\epsilon}\big(e^{\beta\epsilon}-1\big)^{-1}\bigg](\mu_m-\mu_s) \\ &-\frac{g_r^{\uparrow\downarrow}}{\pi s}\int_0^\infty d\epsilon D(\epsilon)(\epsilon-\mu_s)\bigg[\frac{1}{2}\bigg(\beta\frac{\partial}{\partial\epsilon}\big(e^{\beta\epsilon}-1\big)^{-1} - \beta e^{\beta\epsilon}\frac{\partial}{\partial\epsilon}\big(e^{\beta\epsilon}-1\big)^{-2}\bigg)\bigg](\mu_m^2-\mu_s^2) \\ &+\mathcal{O}(\mu^3)\,. \end{aligned}$$

Now because $\mu_s(\mu_m^2-\mu_s^2) = \mathcal{O}(\mu^3)$, these terms can be left out. Then by using Appendix A.3 with the magnon density of states given by $D(\epsilon) = \sqrt{\epsilon}/4\pi^2 J_s^{3/2}$, we get for the accumulation dependent part

$$\begin{aligned} j_{s,\mu}^{int} =& -\frac{g_r^{\uparrow\downarrow}}{\pi s}\bigg(\frac{3\zeta(3/2)}{2\Lambda^3}(\mu_m-\mu_s) - \frac{3\beta\zeta(3/2)}{4\Lambda^3}(\mu_m^2-\mu_s^2)\bigg) \\ &-\frac{g_r^{\uparrow\downarrow}}{\pi s}\int_0^\infty d\epsilon D(\epsilon)\bigg[\frac{\partial}{\partial\epsilon}\big(e^{\beta\epsilon}-1\big)^{-1}\bigg]\mu_s(\mu_m-\mu_s) \qquad (4.5) \\ &-\frac{g_r^{\uparrow\downarrow}}{\pi s}\int_0^\infty d\epsilon D(\epsilon)\epsilon\bigg[-\frac{\beta e^{\beta\epsilon}}{2}\frac{\partial}{\partial\epsilon}\big(e^{\beta\epsilon}-1\big)^{-2}\bigg](\mu_m^2-\mu_s^2) \qquad (4.6) \\ &+\mathcal{O}(\mu^3)\,. \end{aligned}$$

The integrals (4.5) and (4.6) have not yet been evaluated because for the given magnon density of states, proportional to $\sqrt{\epsilon}$, they diverge in their lower limits. This divergence has to be resolved. In Section 3 we expressed the Hamiltonian (3.1) with disregard to any internal as well external magnetic fields. However, as a result of the molecular structure of the magnet there are internal fields present. Also, as a consequence of the electron spin accumulation in the metal near the boundary with the magnet, we have an external field. These fields lead to an extra term in the Hamiltonian that is proportional to the total spin of the magnet. In deriving the eigenenergies of this extended Hamiltonian, we would find in the magnon energy (3.12) a nonzero constant term which we may call Δ. Hence, up to and including first nontrivial order in the wave vector, we can write the magnon energy as $\mathcal{E}_{\mathbf{k}} = \alpha k^2 + \Delta$ where again α is some proportionality constant. The magnon density of states will then be

$$D(\epsilon) = \begin{cases} 0 & \text{if } 0 \le \epsilon < \Delta \\ \dfrac{\sqrt{\epsilon-\Delta}}{4\pi^2 J_s^{3/2}} & \text{if } \epsilon \ge \Delta \end{cases}\,, \tag{4.7}$$

where $\sqrt{\epsilon-\Delta}$ appears as the new radius of the sphere in momentum space. We have that $\Delta \simeq \mu_B B$ where μ_B is the Bohr magneton and B is the magnitude of the magnetic field. For anisotropies in the ferromagnet, one typically has $B \sim B_0 \coloneqq 1$ T so that $\Delta \sim \mu_B B_0$. The dependence of the interfacial spin current on Δ turns out to be only in factors of e^{Δ/k_BT}. Since $\Delta/k_BT \sim \mu_B B_0/k_BT$ and $\mu_B/k_B \sim 1$ K/T we get $\Delta/k_BT \sim T_0/T$ where $T_0 \coloneqq 1$ K so $e^{\Delta/k_BT} \sim e^{T_0/T}$. Generally then $e^{T_0/T} \sim 1$ and we can ignore the temperature dependence of the energy gap. Introducing the energy gap though, lifts the divergence of the integrals (4.5) and (4.6). Inserting the magnon density of states (4.7) gives us for the integral (4.5) that

Figure 9: numerical evaluations of the integrals $I_1(\tilde{\Delta})$ and $I_2(\tilde{\Delta})$. For room temperature $T = 293$ K we find $\tilde{\Delta} \simeq \mu_B B_0/k_BT \simeq 0.0023$. Also note that for $T = 1$ K we get $\tilde{\Delta} \simeq 0.67$ and for $T = 400$ K we get $\tilde{\Delta} \simeq 0.0017$. In this range of $\tilde{\Delta}$ we can safely neglect the temperature dependence of its contribution to the accumulation dependent part of the interfacial spin current.

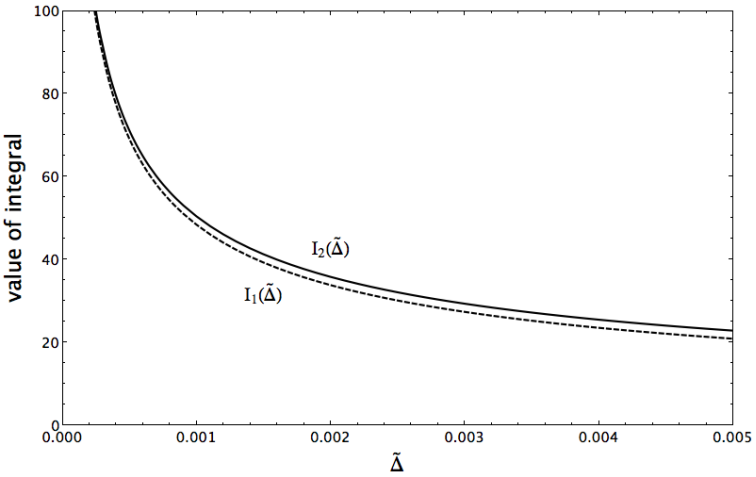

$$\begin{aligned}\int_0^\infty d\epsilon D(\epsilon)\Big[-\frac{\partial}{\partial\epsilon}\big(e^{\beta\epsilon}-1\big)^{-1}\Big] &= -\frac{\beta}{4\pi^2 J_s^{3/2}}\int_\Delta^\infty d\epsilon\big(\epsilon-\Delta\big)^{1/2}\big(e^{\beta\epsilon}-1\big)^{-2}e^{\beta\epsilon}\\ &= -\frac{\beta}{4\pi^2 J_s^{3/2}}\int_0^\infty d\epsilon\epsilon^{1/2}\big(e^{\beta(\epsilon+\Delta)}-1\big)^{-2}e^{\beta(\epsilon+\Delta)}\\ &= -\frac{1}{4\pi^2 J_s^{3/2}\beta^{1/2}}\int_0^\infty dx x^{1/2}\big(e^{x+\tilde{\Delta}}-1\big)^{-2}e^{x+\tilde{\Delta}}\\ &= -\frac{2\beta I_1(\tilde{\Delta})}{\Lambda^3\sqrt{\pi}}\,,\end{aligned}$$

where in the second to last step we substituted $x = \beta\epsilon$ and $\tilde{\Delta} = \beta\Delta$ to have dimensionless parameters making it possible to evaluate numerically $I_1(\tilde{\Delta})$ which we have defined as

$$I_1(\tilde{\Delta}) = \int_0^\infty dx x^{1/2}\big(e^{x+\tilde{\Delta}}-1\big)^{-2}e^{x+\tilde{\Delta}}\,.$$

For the integral in (4.6) we find in the same way as for the integral in (4.5) that

$$\int_0^\infty d\epsilon D(\epsilon)\epsilon\Big[-\frac{\beta e^{\beta\epsilon}}{2}\frac{\partial}{\partial\epsilon}\big(e^{\beta\epsilon}-1\big)^{-2}\Big] = \frac{2\beta I_2(\tilde{\Delta})}{\Lambda^3\sqrt{\pi}}\,,$$

where we have defined $I_2(\tilde{\Delta})$ as

$$I_2(\tilde{\Delta}) = \int_0^\infty dx x^{1/2}(x+\tilde{\Delta})\big(e^{x+\tilde{\Delta}}-1\big)^{-3}e^{2(x+\tilde{\Delta})}\,.$$

A plot of the numerically evaluated integrals $I_1(\tilde{\Delta})$ and $I_2(\tilde{\Delta})$ can be found in Figure 9. We can now give a final expression for the accumulation dependent part of the interfacial spin current up to and including second order in the accumulations:

$$j_{s,\mu}^{int} = -\frac{g_r^{\uparrow\downarrow}}{\pi s \Lambda^3}\left\{\frac{3\zeta(3/2)}{2}(\mu_m - \mu_s) - \frac{2\beta I_1(\tilde{\Delta})}{\sqrt{\pi}}\mu_s(\mu_m - \mu_s) + \left(\frac{2\beta I_2(\tilde{\Delta})}{\sqrt{\pi}} - \frac{3\beta\zeta(3/2)}{4}\right)(\mu_m^2 - \mu_s^2)\right\} + \mathcal{O}(\mu^3)\,.$$

In Section 5 we add the equation of the interfacial spin current (which will look like $j_{s,\mu}^{int}$ since we will assume $T_e = T_m$) to the equations of the charge current j_c, the electron spin current j_s^e and the magnon spin current j_s^m given in Subsections 4.1 and 4.2. This allows us to solve for the spin accumulation μ_s and magnon accumulation μ_m whose functional forms are determined by their accompanying diffusion equations.

5 Unidirectional spin Hall magnetoresistance

In Subsection 5.1 we find an explicit expression for the unidirectional spin Hall magnetoresistance. Before finding such an expression, we first explain this effect qualitatively by considering what happens when we place a ferromagnetic insulator on top of a nonmagnetic metal. Then in Subsection 5.2 we replace parameters with numerical values corresponding to a bilayer of platinum and yttrium iron garnet. This allows us to consider the dependence of the USMR on the thickness of the ferromagnet and on the temperature.

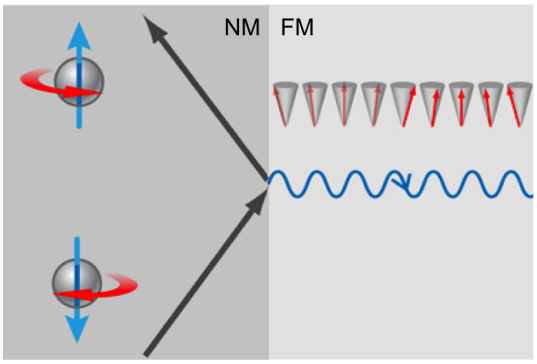

Figure 10: microscopical representation of the conversion of an electron spin current into a magnon spin current at the boundary between a nonmagnetic metal and a ferromagnetic insulator. Reprinted from Reference [17].

5.1 Phenomenology of the USMR

Due to the spin Hall effect, when a charge current flows parallel to the boundary of a metal, a spin current carried by valence electrons flows perpendicular to this boundary. Since the electrons can not flow out of the metal, electron spins of corresponding orientation accumulate near the boundary. The generated spin concentration gradient causes spins of equal orientation to diffuse, following the spin diffusion equation given in Subsection 4.1. The opposing flow of electron spins impedes further accumulation of spin until an equilibrium is attained (cf. the classical Hall effect in Subsection 2.1).

When we put a ferromagnetic insulator on top of this nonmagnetic metal, the following happens. Although the electrons can not flow out of the metal and into the magnetic insulator, the electron spin current can be converted into a magnon spin current at the interface of the bilayer. Microscopically, an electron spin that reaches the interface will flip its orientation creating a magnon (by conservation of angular momentum)

Figure 11: interacting charge and spin currents. In (a) we have the spin Hall effect where the longitudinal charge current is converted into the transverse spin current. In (b) we see the inverse spin Hall effect where the longitudinal spin current is converted into the transverse charge current. Reprinted from Reference [18].

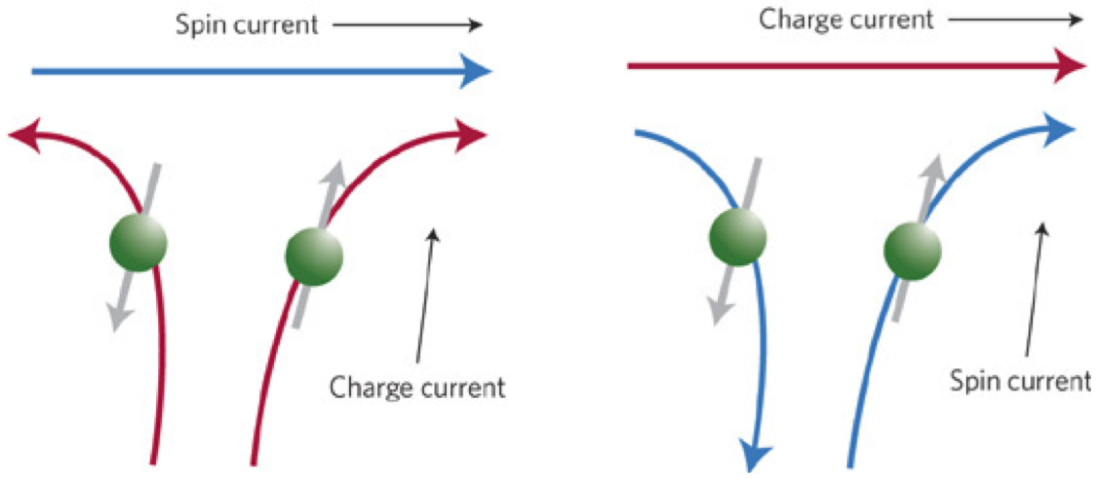

(a) **(b)**

Figure 12: nonlinear character of the USMR. In (a) we have a parallel alignment of the magnetization of the ferromagnet with the magnetization at the interface induced by the spin Hall effect. This leads to a high resistance. In (b) we have an antiparallel alignment of such, leading to a low resistance. Reprinted from Reference [1].

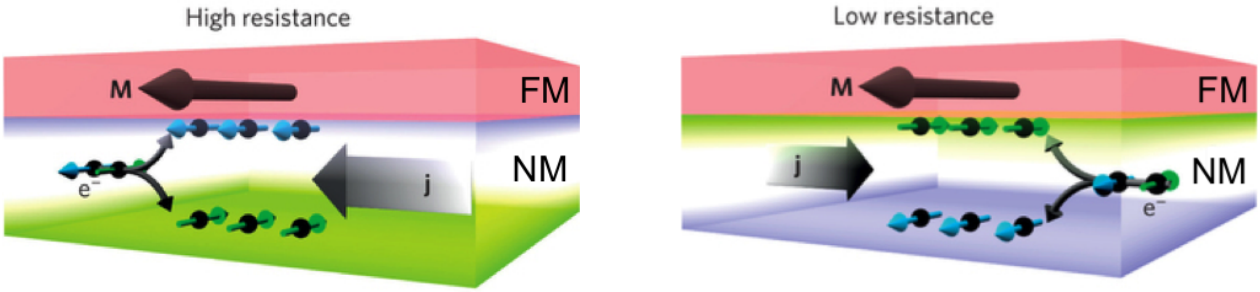

(a) **(b)**

in the ferromagnet (see Figure 10). In the magnet, following the magnon spin diffusion equation given in Subsection 4.2, the magnons diffuse and then relax according to the magnon relaxation length. This magnon relaxation thus results in a dissipation of the electron spin current into the ferromagnet.

Limiting our attention to only the nonmagnetic metal, this dissipation of the electron spin current into the magnet can be interpreted as a small effective spin current in the metal. The effective spin current will be in the same direction as the electron spin current induced by the initial charge current. For example, say that spin down electrons accumulate near the interface. By creating a magnon, these electron spins flip, changing their spin from down to up. The extra spin up electrons now created, diffuse away from the interface. Hence a spin current starts to flow in the same direction as that of the one we began with. By the inverse spin Hall effect (see Figure 11 for a qualitative understanding of this effect), the effective spin current in the metal induces a charge current opposite to the direction of the original charge current. The resulting resistance is known as the unidirectional spin Hall magnetoresistance (USMR).

Still we have not yet made mention of the nonlinear character of the USMR. The nonlinear dependence of the USMR on the direction of the electric field appears as a result of the spin Hall effect. Depending on the direction of the electric field, either spin down or spin up electrons accumulate near the interface. Since the magnetization direction of the ferromagnetic layer is fixed, these spins are either parallel or antiparallel to this magnetization. It turns out from the experiments performed by Avci *et al.* that a parallel alignment leads to a high resistance whereas an antiparallel alignment leads to a low resistance (see Figure 12).

Having explained the USMR and its nonlinear character, we now set out to find the magnon contribution. We first summarize results. Putting all the different currents together and considering only the accumulation dependent part of the interfacial spin current, we have

$$j_c = \sigma E + \frac{\sigma\theta}{2e}\frac{\partial \mu_s}{\partial z}\,, \tag{5.1}$$

$$j_s^e = \frac{\hbar}{2e}\Big(- \frac{\sigma}{2e}\frac{\partial \mu_s}{\partial z} - \sigma\theta E\Big)\,, \tag{5.2}$$

$$j_s^m = -\frac{\sigma_m}{\hbar}\frac{\partial \mu_m}{\partial z}\,, \tag{5.3}$$

$$\begin{aligned} j_s^{int} = -\frac{g_r^{\uparrow\downarrow}}{\pi s \Lambda^3}\Bigg\{ &\frac{3\zeta(3/2)}{2}(\mu_m - \mu_s) - \frac{2\beta I_1(\tilde{\Delta})}{\sqrt{\pi}}\mu_s(\mu_m - \mu_s) \\ &+ \left(\frac{2\beta I_2(\tilde{\Delta})}{\sqrt{\pi}} - \frac{3\beta\zeta(3/2)}{4}\right)(\mu_m^2 - \mu_s^2)\Bigg\} + \mathcal{O}(\mu^3)\,. \end{aligned} \tag{5.4}$$

For our purpose we need to know the charge current. Therefore, the equations above must first be solved for the accumulations μ_s and μ_m. Following the diffusion equations, these accumulations generically look like

$$\frac{\partial^2\mu_s}{\partial z^2} = \frac{\mu_s}{l_s^2} \qquad \Rightarrow \qquad \mu_s = Ae^{z/l_s} + Be^{-z/l_s}\,, \tag{5.5}$$

$$\frac{\partial^2\mu_m}{\partial z^2} = \frac{\mu_m}{l_m^2} \qquad \Rightarrow \qquad \mu_m = Ce^{z/l_m} + De^{-z/l_m}\,, \tag{5.6}$$

where A, B, C and D are unknown constants. Introducing the thickness of the nonmagnetic metal L_{NM} and that of the ferromagnetic insulator L_{FM} and placing the interface between the metal and the ferromagnet at $z = 0$, we impose the following four boundary conditions

$$j_s^e(-L_{NM}) = 0\,, \tag{5.7}$$

$$j_s^m(L_{FM}) = 0\,, \tag{5.8}$$

$$j_s^e(0) = j_s^m(0)\,, \tag{5.9}$$

$$j_s^e(0) = j_s^{int}(0)\,, \tag{5.10}$$

which allow us to find the unknowns and hence find expressions for the accumulations. The first boundary condition (5.7) states that the spin current carried by the valence electrons in the nonmagnetic metal induced by the spin Hall effect must be zero at the boundary of the metal opposite to the interface with the ferromagnet (i.e. no current can flow out of the metal). The second boundary condition (5.8) says that the magnon spin current injected into the ferromagnetic insulator must be zero at the boundary of the ferromagnet opposite to the interface with the metal (i.e. no current can flow out of the magnet). Boundary condition (5.9) makes sure that the spin currents directly on both sides of the interface are equal. The final boundary condition (5.10) ensures that both these currents are equal to the interfacial spin current.

Now, just as we made the integrals (4.5) and (4.6) dimensionless in order to be able to evaluate them numerically, we have to make the equations (5.1)-(5.4), the accumulations (5.5) and (5.6) and the boundary conditions (5.7)-(5.10) dimensionless to solve them numerically.

We divide j_c by $j_c^0 = \sigma|E|$ yielding $\tilde{j}_c = j_c/j_c^0$ and divide j_s^e, j_s^m and j_s^{int} by $j_s^0 = \frac{\hbar}{2e}j_c^0 = \frac{\hbar}{2e}\sigma|E|$ yielding $\tilde{j}_s^e = j_s^e/j_s^0$, $\tilde{j}_s^m = j_s^m/j_s^0$ and $\tilde{j}_s^{int} = j_s^{int}/j_s^0$. In addition we introduce $\tilde{\mu}_s = \mu_s/e|E|l_s$ and $\tilde{\mu}_m = \mu_m/e|E|l_m$. Also we will use $z_s = z/l_s$ and $z_m = z/l_m$. Implementing all of this, the equations (5.1)-(5.4) become

$$\begin{aligned}
\tilde{j}_c &= \frac{E}{|E|} + \frac{\theta}{2}\frac{\partial\tilde{\mu}_s}{\partial z_s}\,,\\
\tilde{j}_s^e &= -\frac{1}{2}\frac{\partial\tilde{\mu}_s}{\partial z_s} - \frac{E}{|E|}\theta\,,\\
\tilde{j}_s^m &= -\frac{2e^2}{\hbar^2}\frac{\sigma_m}{\sigma}\frac{\partial\tilde{\mu}_m}{\partial z_m}\,,\\
\tilde{j}_s^{int} &= -\frac{g_r^{\uparrow\downarrow}}{\pi s\Lambda^3}\frac{2e^2}{\sigma\hbar}\left\{\frac{3\zeta(3/2)}{2}(l_m\tilde{\mu}_m - l_s\tilde{\mu}_s) - \frac{2\beta e|E|I_1(\tilde{\Delta})}{\sqrt{\pi}}l_s\tilde{\mu}_s(l_m\tilde{\mu}_m - l_s\tilde{\mu}_s)\right.\\
&\quad\left. + \left(\frac{2\beta e|E|I_2(\tilde{\Delta})}{\sqrt{\pi}} - \frac{3\beta e|E|\zeta(3/2)}{4}\right)(l_m^2\tilde{\mu}_m^2 - l_s^2\tilde{\mu}_s^2)\right\} + \mathcal{O}(\mu^3)\,.
\end{aligned}$$

with the dimensionless accumulations given by

$$\frac{\partial^2\tilde{\mu}_s}{\partial z_s^2} = \tilde{\mu}_s \qquad \Rightarrow \qquad \tilde{\mu}_s = \tilde{A}e^{z_s} + \tilde{B}e^{-z_s}\,,$$
$$\frac{\partial^2\tilde{\mu}_m}{\partial z_m^2} = \tilde{\mu}_m \qquad \Rightarrow \qquad \tilde{\mu}_m = \tilde{C}e^{z_m} + \tilde{D}e^{-z_m}\,,$$

where simply $\tilde{A} = A/e|E|l_s$, $\tilde{B} = B/e|E|l_s$, $\tilde{C} = C/e|E|l_m$ and $\tilde{D} = A/e|E|l_m$. These dimensionless unknowns are then to be found under constraints of

$$\tilde{j}_s^e(-L_{NM}/l_s) = 0\,,$$
$$\tilde{j}_s^m(L_{FM}/l_m) = 0\,,$$
$$\tilde{j}_s^e(0) = \tilde{j}_s^m(0)\,,$$
$$\tilde{j}_s^e(0) = \tilde{j}_s^{int}(0)\,.$$

Using a computer we can express $\tilde{A}$, $\tilde{B}$, $\tilde{C}$ and $\tilde{D}$ in terms of all the parameters that have so far been introduced. One might guess that these expressions are lengthy and this guess would be correct. In order to say anything sensible then, we have to put numbers in for these parameters. This is what we do in Subsection 5.2 where we consider a bilayer of platinum and yttrium iron garnet (denoted as Pt/YIG). Before we do so however, we first explain how to find the unidirectional spin Hall magnetoresistance from the now known accumulations.

Having computed the interfacial spin current up to and including second order in the accumulations and having solved for the spin accumulation μ_s, we can write the charge current j_c (5.1) by an expansion in the electric field as

$$j_c(z) = \sigma^{(0)}(z)E + \sigma^{(1)}(z)E^2\,, \tag{5.11}$$

where it is known (at least hypothetically) what $\sigma^{(0)}$ and $\sigma^{(1)}$ look like as functions of z. To get rid of the dependence on z we integrate the charge current j_c in (5.11) over the thickness of the nonmagnetic metal and divide this by the same length to find the averaged out charge current

$$I = \frac{1}{L_{NM}}\int_0^{L_{NM}} dz j_c(z)\,,$$

acknowledging that throughout we have called j_c the charge current where in fact it is a charge current *density*. Factoring out E from (5.11) we see that we can write

$$I = \sigma(E)E\,,$$

where $\sigma(E)$ is simply the sum of $\sigma^{(0)}(z)$ and $\sigma^{(1)}(z)E$ averaged out over the thickness of the nonmagnetic metal. Introducing the longitudinal resistivity of the metal $\rho(E) = 1/\sigma(E)$ which straightforwardly looks like

$$\rho = \frac{L_{NM}E}{\int_0^{L_{NM}} dz j_c(z)}\,,$$

Table 1: values and expressions for selected parameters. Here room temperature is 293 K. The numerical values and the expressions come from References [7, 15].

	Symbol	Value	Unit	Expression
Platinum spin relaxation length	l_s	1.5	nm	
Platinum conductivity	σ	0.1×10^8	$(\Omega\ \mathrm{m})^{-1}$	
Platinum spin Hall angle	θ	0.11		
YIG spin-wave stiffness constant	J_s	8.458×10^{-40}	J m^2	
Magnon thermal velocity	v_{th}		$\sim$ km s^{-1}	$v_{th} = \frac{2\sqrt{J_s k_B T}}{\hbar}$
Gilbert damping constant	α	10^{-4}		
YIG magnon relaxation time	τ_{mr}		$\sim$ ns	$\tau_{mr} = \frac{\hbar}{2\alpha k_B T}$
YIG magnon relaxation length	l_m		$\sim \mu$m	$l_m = v_{th}\sqrt{\frac{2}{3}\tau_{mr}\left(\frac{1}{\tau_{el}} + \frac{1}{\tau_{mr}}\right)^{-1}}$
Thermal de Broglie wavelength at room temperature	Λ	1.6	nm	$\Lambda = \sqrt{4\pi J_s / k_B T}$
YIG magnon spin conductivity at room temperature	σ_m	1.4×10^{-22}	J s m^{-1}	$\sigma_m = \frac{2\zeta(3/2) J_s}{\Lambda^3}\left(\frac{1}{\tau_{el}} + \frac{1}{\tau_{mr}}\right)^{-1}$
Spin quantum number per YIG unit cell	S	10		
YIG lattice constant	a	12.376	Å	
YIG equilibrium spin density	s	5.2754×10^{-3}	Å^{-3}	$s = S/a^3$
Real part of the spin-mixing conductance	$g_r^{\uparrow\downarrow}$	5×10^{18}	m^{-2}	

we can now characterize the amplitude of the unidirectional spin Hall magnetoresistance by the ratio

$$\mathrm{USMR} = \frac{\rho(E) - \rho(-E)}{\rho(E)}\,.$$

In Subsection 5.2 we consider a Pt/YIG bilayer to be able to substitute numerical values for the parameters on which the USMR depends. In this way we can find the dependence of the USMR on the thickness of the ferromagnetic layer and on the temperature.

5.2 Pt/YIG

In this Subsection we replace the parameters with the numerical values given in Table 1. These are values corresponding to a Pt/YIG bilayer. In addition we consider a platinum layer of thickness $L_{NM} = 15$ nm (which is several times the platinum spin relaxation length) and an electric field $|E| = 10^5$ N/C, which corresponds to charge current densities $j_c = 10^7 - 10^8$ A cm^{-2} as used by Avci *et al.* [1]. We evaluate the integrals $I_1(\tilde{\Delta})$ and $I_2(\tilde{\Delta})$, their temperature dependence being of no concern, at $\tilde{\Delta} = 0.0023$ for computational convenience (see Figure 9).

First we look at how the USMR depends on the thickness of the ferromagnet. Then finally we discuss the USMR as a function of temperature. In both cases, we introduce the elastic relaxation time τ_{el} which considers the elastic magnon scattering by bulk impurities or interface disorders. We first work in the limit of a clean system where $\tau_{el} \to \infty$. Then we consider some values for τ_{el} knowing that $\tau_{el} \sim 0.1 - 1$ ps [15].

Figure 13: USMR versus the ratio of the thickness of the ferromagnet to the magnon spin relaxation length. In (a) we work under the assumption of a clean system. We see that at first the USMR gets bigger for a thicker ferromagnetic layer. Then after approximately twice the relaxation length, the USMR has saturated. In (b) we have plotted the USMR for different values of the elastic relaxation time.

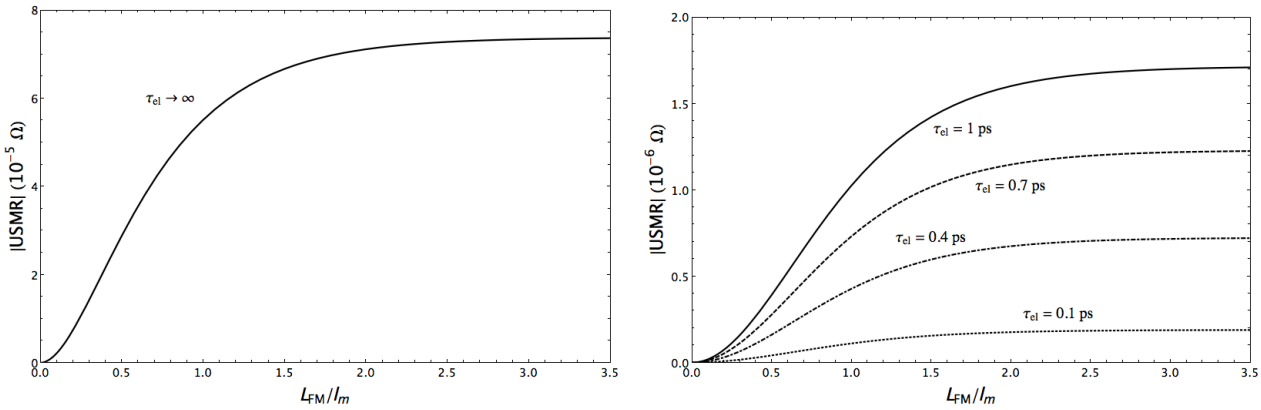

Figure 14: USMR versus the temperature. In (a) we work under the assumption of a clean system. At first the USMR increases with increasing temperatures. Then, after a certain temperature, the USMR starts to slightly decrease. In (b) we have plotted the USMR for different values of the elastic relaxation time.

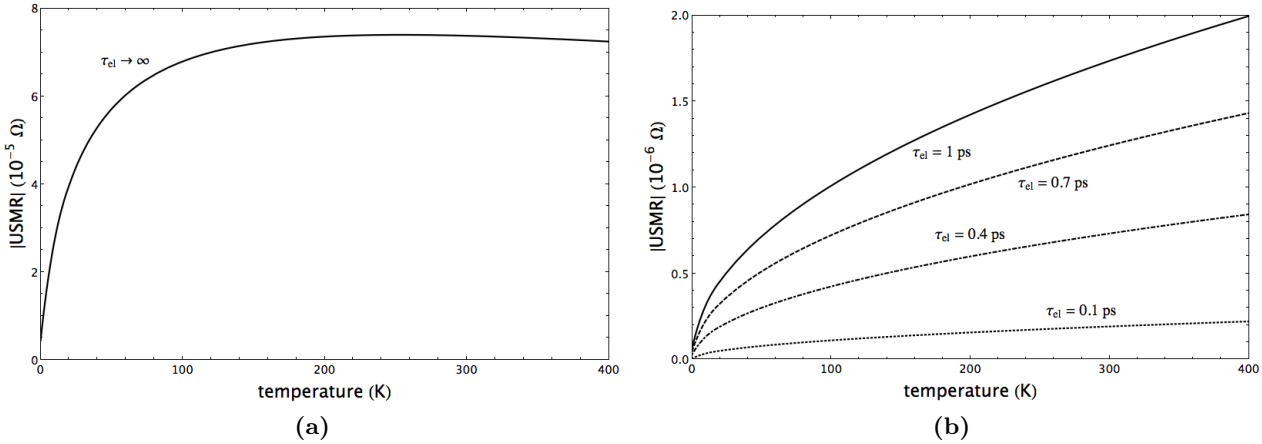

5.2.1 Dependence USMR on thickness ferromagnet

For the dependence of the USMR on the thickness of the ferromagnetic insulator YIG, we still need to fix the temperature. We take the temperature to be room temperature i.e. $T = 293$ K. With all the parameters now given a numerical value, apart from the thickness of the ferromagnet L_{FM}, we find a dependence as is depicted in Figure 13. In all cases, we naturally have that if there is no ferromagnetic layer (i.e. $L_{FM} = 0$) then the USMR is absent.

Looking at Figure 13a, we see that after approximately two times the YIG magnon spin relaxation length l_m the USMR has saturated. Such a saturation of the USMR with increasing thickness of the ferromagnetic layer was to be expected. The magnitude of the USMR has to do with the dissipation of the electron spin current into the magnet. This dissipation comes from the relaxation of the magnons. After a couple magnon spin relaxation lengths then, this dissipation does not grow any larger as the thickness of the ferromagnetic layer increases.

In Figure 13b we have dropped the approximation of a clean system and substituted some values for the elastic relaxation time. We see that the introduction of a finite τ_{el} (in addition to the scattering due to magnon-phonon interactions that annihilate or create spin waves modelled by τ_{mr}) reduces the magnitude of the USMR by one order.

5.2.2 Dependence USMR on temperature

For the dependence of the USMR on the temperature, we still have to specify the thickness of the ferromagnetic layer. We take this layer to be of thickness $L_{FM} = 94$ μm (which is several times the YIG magnon relaxation length). Having specified all the parameters, apart from the temperature T, we find a dependence as is depicted in Figure 14. We see in all cases that at zero temperature, the USMR is zero as well. Since at zero temperature all the spins simply align in the ferromagnetic ground state and hence there will be no magnons, this should indeed be so.

Looking at Figure 14a, we see that increasing the temperature first leads to a steep increase of the USMR. This corresponds to the fact that at nonzero temperatures magnons can arise and hence the spin current from the valence electrons in the metal will be able to dissipate into the ferromagnet. Further increasing the temperature eventually leads to the USMR starting to slightly decrease. For a discussion on this behaviour, we refer to Section 6.

In Figure 14b we have dropped the approximation of a clean system and substituted some values for the elastic relaxation time. Again we see that the introduction of a finite τ_{el} reduces the magnitude of the USMR by one order. Also we note that by the introduction of this relaxation time, the USMR is suppressed less with increasing temperature. We refer to Section 6 for a discussion.

6 Discussion

In Section 1 we introduced the field of spintronics and the concept of magnons. In recent research by Avci *et al.* [1] in this field, measurements were made of a unidirectional spin Hall magnetoresistance. This was an unusual result since normally magnetoresistive effects are invariant on inversion of the magnetization direction. Zhang and Vignale [2] considered only the electronic contribution to the USMR in order to explain its nonlinear behaviour quantitatively. They accounted for half the experimental value measured. It was our attempt to consider the magnon contribution to the USMR.

A comparison of orders

Unexpectedly, the contribution of magnons to the USMR leads to a same order of magnitude of the USMR as the electronic contribution. A priori, we predicted the magnon contribution to lead to lower orders of magnitude of the USMR than the electronic contribution. In Reference [2], Zhang and Vignale obtain an expression for the USMR of $\mathcal{O}(\theta)$. From the equation (4.4) we can infer that the magnon contribution to the USMR is of $\mathcal{O}(\theta^3)$ in the following way. Given an electron spin accumulation at the interface $\mu_s(0)$ and together with the magnon diffusion equation (5.6), the equation (4.4) leads to a magnon accumulation $\mu_m(0)$ at the interface that depends nonlinearly on $\mu_s(0)$. Plugging this $\mu_m(0)$ in the expression for the spin current across the interface (4.1) and setting $T_e = T_m$, we obtain for the interfacial spin current

$$j_s^{int} = \left(\frac{\partial j_s^{int}}{\partial \mu_s}\right)\mu_s(0) + \left(\frac{\partial^2 j_s^{int}}{\partial \mu_s^2}\right)(\mu_s(0))^2\,,$$

where higher order terms in $\mu_s(0)$ are omitted. Since $\mu_s(0)$ is of $\mathcal{O}(\theta)$, the terms in the above equation are of $\mathcal{O}(\theta)$ and $\mathcal{O}(\theta^2)$. Because $\mu_s(0) \propto E$, only the term proportional to $(\mu_s(0))^2$ contributes to the USMR. The contribution of this term to the USMR is one power in θ higher because of the conversion from spin to charge current. Hence we can conclude that the contribution of magnons to the USMR is $\mathcal{O}(\theta^3)$. Since θ is a small parameter, we expected the magnon contribution to be of less impact on the USMR than the electron contribution. Somewhere however, the difference of $\mathcal{O}(\theta^2)$ between the two is compensated for. This makes that the magnon contribution to the USMR can not be neglected.

It raises the question what happens if we combine the contribution of the electrons and of the magnons. One thing that could happen, is that we get two saturation levels when we plot the USMR against the length of our system (see Figure 15). The first saturation then comes from the electron spin relaxation length l_s and the second from the magnon spin relaxation length l_m. This is because typically $l_s \sim$ nm and $l_m \sim \mu$m. We note however that the two levels will only be distinguishable when the electron and magnon spin relaxation length are far enough apart.

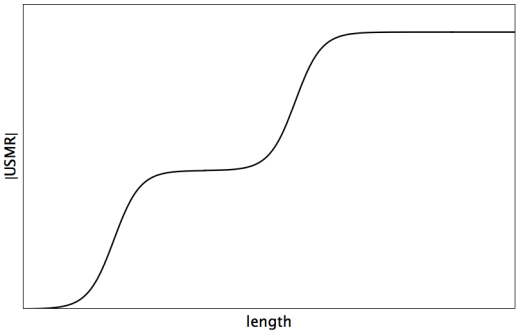

Figure 15: schematic illustration of the double saturation of the USMR as a function of length when both electrons and magnons are taken into account.

A decrease of USMR(T)

The second interesting thing that follows from our results is that the USMR as a function of temperature starts to decrease, albeit slowly, from a certain temperature on (see Figure 14a). This means there is some temperature dependent parameter in the equations suppressing the USMR. Taking a look at Table 1, we see

that there really are only three candidates: the thermal de Broglie wavelength Λ, the magnon spin relaxation length l_m and the magnon spin conductivity σ_m.

The thermal de Broglie wavelength actually makes the USMR increase as a function of temperature in the first place. It appears as Λ^{-3} in the interfacial spin current and since $\Lambda^{-3} \sim T^{3/2}$, even when multiplied by β, it is still a positive power of T. Also, the decrease of the USMR can not come from the magnon spin relaxation length. Namely, increasing the temperature leads to a smaller relaxation length which leads to a bigger ratio L_{FM}/l_m. The bigger this ratio, the bigger the USMR (see Figure 13). Hence it can never be that the relaxation length makes the USMR decrease as a function of temperature. The only temperature dependence then left in the parameters is that of the magnon spin conductivity through the magnon relaxation time τ_{mr}. Indeed, if we fix the temperature for τ_{mr}, the USMR is seen to increase. A possible determination of the maximum is left for future study.

The suppression of the USMR due to the temperature dependence of τ_{mr} also explains why the introduction of a finite τ_{el} decreases the USMR suppression with increasing temperature (cf. Figures 14a and 14b). By adding a relaxation time independent of temperature, the temperature dependence of τ_{mr} fails to have a visual effect on the USMR.

Approximations

Throughout we have made several approximations. First of all, in deriving an expression for the interfacial spin current we neglected its temperature dependent part altogether by setting $T_e = T_m$. In reality though, $T_e \neq T_m$ because of the different thermal properties of the two materials. An improvement of our work would thus be the inclusion of the temperature dependent part of the interfacial spin current.

Second, in calculating the USMR in a Pt/YIG bilayer configuration we did not include the temperature dependence of $\tilde{\Delta}$. Although for most temperatures this dependence is negligible, as it appears only in the interfacial spin current as $e^{\tilde{\Delta}} \sim e^{T_0/T}$, for low temperatures it may give a slight correction on our results.

Finally, we took the static magnetization direction of the ferromagnet $\hat{\mathbf{n}}$ to be in the positive y-direction i.e. we set $\hat{\mathbf{n}} = \hat{\mathbf{y}}$. A generalization would be to fix the average magnetization direction of the ferromagnet in an arbitrary direction.

A Appendix

A.1 Taylor expansion in ΔT

Here we explicitly compute the different terms of the Taylor expansion in ΔT of the Bose-Einstein function:

$$\begin{aligned} n_B\left(\frac{\epsilon}{k_B(T_e-\Delta T)}\right) - n_B\left(\frac{\epsilon}{k_B T_e}\right) =& \left[\left(e^{\epsilon/k_B(T_e-\Delta T)}-1\right)^{-1} - \left(e^{\epsilon/k_B T_e}-1\right)^{-1}\right]_{\Delta T=0} \\ &+ \left[\frac{\partial}{\partial(\Delta T)}\left(e^{\epsilon/k_B(T_e-\Delta T)}-1\right)^{-1}\right]_{\Delta T=0}\Delta T \\ &+ \mathcal{O}\big[(\Delta T)^2\big]\,. \end{aligned}$$

The linear term, evaluated at $\Delta T = 0$, then is

$$\begin{aligned} &\left[\frac{\partial}{\partial(\Delta T)}\left(e^{\epsilon/k_B(T_e-\Delta T)}-1\right)^{-1}\right]_{\Delta T=0} \\ &= \left[-\left(e^{\epsilon/k_B(T_e-\Delta T)}-1\right)^{-2} e^{\epsilon/k_B(T_e-\Delta T)}\frac{\epsilon}{k_B(T_e-\Delta T)^2}\right]_{\Delta T=0} \\ &= -\frac{\epsilon}{k_B T_e^2} e^{\epsilon/k_B T_e}\left(e^{\epsilon/k_B T_e}-1\right)^{-2} \\ &= \frac{\epsilon}{T_e}\frac{\partial}{\partial\epsilon}\left(e^{\epsilon/k_B T_e}-1\right)^{-1}. \end{aligned}$$

A.2 Taylor expansion in μ

Here we explicitly compute the different terms of the Taylor expansion in μ of the Bose-Einstein function:

$$n\big(\beta(\epsilon-\mu)\big) = n\big(\beta(\epsilon-\mu)\big)\Big|_{\mu=0} + \frac{\partial}{\partial\mu}n\big(\beta(\epsilon-\mu)\big)\Big|_{\mu=0}\mu + \frac{1}{2}\frac{\partial^2}{\partial\mu^2}n\big(\beta(\epsilon-\mu)\big)\Big|_{\mu=0}\mu^2 + \mathcal{O}\big(\mu^3\big)\,.$$

The linear term, evaluated at $\mu = 0$, then is

$$\begin{aligned} \frac{\partial}{\partial\mu}n\big(\beta(\epsilon-\mu)\big)\Big|_{\mu=0} &= \beta e^{\beta(\epsilon-\mu)}\left(e^{\beta(\epsilon-\mu)}-1\right)^{-2}\Big|_{\mu=0} \\ &= \beta e^{\beta\epsilon}\left(e^{\beta\epsilon}-1\right)^{-2} \\ &= -\frac{\partial}{\partial\epsilon}\left(e^{\beta\epsilon}-1\right)^{-1}. \end{aligned}$$

The quadratic term, evaluated at $\mu = 0$, then is

$$\begin{aligned}\frac{\partial^2}{\partial\mu^2}n\big(\beta(\epsilon-\mu)\big)\Big|_{\mu=0} &= \Big(-\beta^2 e^{\beta(\epsilon-\mu)}\big(e^{\beta(\epsilon-\mu)}-1\big)^{-2}+2\beta^2 e^{2\beta(\epsilon-\mu)}\big(e^{\beta(\epsilon-\mu)}-1\big)^{-3}\Big)\Big|_{\mu=0}\\ &= \Big(-\beta^2 e^{\beta\epsilon}\big(e^{\beta\epsilon}-1\big)^{-2}+2\beta^2 e^{2\beta\epsilon}\big(e^{\beta\epsilon}-1\big)^{-3}\Big)\Big|_{\mu=0}\\ &= \beta\frac{\partial}{\partial\epsilon}\big(e^{\beta\epsilon}-1\big)^{-1}-\beta e^{\beta\epsilon}\frac{\partial}{\partial\epsilon}\big(e^{\beta\epsilon}-1\big)^{-2}.\end{aligned}$$

A.3 A typical integral

In this Appendix we evaluate an integral that we encounter several times throughout Section 4. If we take $n \geq 1$ a natural number then

$$\begin{aligned}&\int_0^\infty d\epsilon\epsilon^{n+\frac{1}{2}}\left[\frac{\partial}{\partial\epsilon}\big(e^{\beta\epsilon}-1\big)^{-1}\right]\\ &\overset{\text{P.I.}}{=}\left[\epsilon^{n+\frac{1}{2}}\big(e^{\beta\epsilon}-1\big)^{-1}\right]_0^\infty-\int_0^\infty d\epsilon\big(e^{\beta\epsilon}-1\big)^{-1}\left[\frac{\partial}{\partial\epsilon}\epsilon^{n+\frac{1}{2}}\right]\\ &=\left[\lim_{\epsilon\to\infty}\epsilon^{n+\frac{1}{2}}\big(e^{\beta\epsilon}-1\big)^{-1}-\lim_{\epsilon\to0}\epsilon^{n+\frac{1}{2}}\big(e^{\beta\epsilon}-1\big)^{-1}\right]-\int_0^\infty d\epsilon\big(e^{\beta\epsilon}-1\big)^{-1}\left[\Big(n+\frac{1}{2}\Big)\epsilon^{n-\frac{1}{2}}\right]\\ &\overset{\text{l'Hôpital}}{=}-\lim_{\epsilon\to0}\Big(n+\frac{1}{2}\Big)\epsilon^{n-\frac{1}{2}}\big(\beta e^{\beta\epsilon}\big)^{-1}-\Big(n+\frac{1}{2}\Big)\int_0^\infty d\epsilon\big(e^{\beta\epsilon}-1\big)^{-1}\epsilon^{n-\frac{1}{2}}\\ &\overset{x=\beta\epsilon}{=}-\Big(n+\frac{1}{2}\Big)\beta^{-(n+\frac{1}{2})}\int_0^\infty dx\big(e^x-1\big)^{-1}x^{n-\frac{1}{2}}\\ &=-\Big(n+\frac{1}{2}\Big)\beta^{-(n+\frac{1}{2})}\Gamma(n+\tfrac{1}{2})\zeta(n+\tfrac{1}{2}),\end{aligned}$$

where $\zeta(s)$ is the Riemann zeta function with s a complex variable and $\Gamma(z)$ is the gamma function with z a complex number that is not a non-positive integer. In the first step we partially integrated, getting rid of the derivative in the square brackets. In the third step we used L'Hôpital's rule to evaluate the lower limit (where the upper limit simply yields a zero value). In the second to last step we made the substitution $x = \beta\epsilon$. Note that if $n < 1$ then applying L'Hôpital's rule does not resolve the limit to infinity, which is why we have to introduce the energy gap Δ.

References

[1] Avci, C. O., Garello, K., Ghosh, A., Gabureac, M., Alvarado, S. F., & Gambardella, P. (2015). Unidirectional spin Hall magnetoresistance in ferromagnet/normal metal bilayers. *Nature Physics, 11*(7), 570-575.

[2] Zhang, S. S. L., & Vignale, G. (2016). Theory of unidirectional spin Hall magnetoresistance in heavy-metal/ferromagnetic-metal bilayers. *Physical Review B, 94*(14), 140411.

[3] Bardeen, J., & Brattain, W. H. (1948). The transistor, a semi-conductor triode. *Physical Review, 74*(2), 230.

[4] Moore, G. E. (1998). Cramming more components onto integrated circuits. *Proceedings of the IEEE, 86*(1), 82-85.

[5] Moore, G. E. (2006). Progress in digital integrated electronics [Technical literaiture, copyright 1975 IEEE. reprinted, with permission. technical digest. international electron devices meeting, IEEE, 1975, pp. 11-13.]. *IEEE Solid-State Circuits Society Newsletter, 20*(3).

[6] Petrucci, R. H. (2007). *General chemistry: Principles and modern applications*. Upper Saddle River, N.J: Pearson/Prentice Hall.

[7] Peters, K.J.H. (2015). Magnon-mediated current drag in the semiclassical regime. *Bachelor thesis*, Utrecht University.

[8] Drude, P. (1900). Zur elektronentheorie der metalle. *Annalen der Physik, 306*(3), 566-613.

[9] Ashcroft, N. W., & Mermin, N. D. (1976). *Solid state physics*. New York: Holt, Rinehart and Winston.

[10] Chudnovsky, E. M. (2007). Theory of spin Hall effect: Extension of the Drude model. *Physical review letters, 99*(20), 206601.

[11] Hall, E. H. (1879). On a new action of the magnet on electric currents. *American Journal of Mathematics, 2*(3), 287-292.

[12] Kittel, C. (2005). *Introduction to solid state physics*. Hoboken, NJ: Wiley.

[13] Dyakonov, M. I., & Perel, V. I. (1971). Current-induced spin orientation of electrons in semiconductors. *Physics Letters A, 35*(6), 459-460.

[14] Heisteeg, D.T.E. van de (2016). Quantum fluctuations and phase transitions in antiferromagnetic spin configurations. *Bachelor thesis*, Utrecht University.

[15] Cornelissen, L. J., Peters, K. J., Bauer, G. E., Duine, R. A., & van Wees, B. J. (2016). Magnon spin transport driven by the magnon chemical potential in a magnetic insulator. *Physical Review B, 94*(1), 014412.

[16] Bender, S. A., & Tserkovnyak, Y. (2015). Interfacial spin and heat transfer between metals and magnetic insulators. Physical Review B, 91(14), 140402.

[17] Kajiwara, Y., Harii, K., Takahashi, S., Ohe, J., Uchida, K., Mizuguchi, M., ... & Maekawa, S. (2010). Transmission of electrical signals by spin-wave interconversion in a magnetic insulator. *Nature, 464*(7286), 262-266.

[18] Maekawa, S. (2009). Magnetism: A flood of spin current. *Nature materials, 8*(10), 777-778.